This is to certify that the
dissertation entitled

MATHEMATICAL ANALYSIS OF MULTICAPILLARY SUPPLY REGION

presented by

Liang Sun

has been accepted towards fulfillment
of the requirements for the

Doctoral degree in Applied Mathematics

C Y Wang
Major Professor's Signature

12/4/08
Date

MATHEMATICAL ANALYSIS OF MULTICAPILLARY SUPPLY REGION

By

Liang Sun

A DISSERTATION

Submitted to
Michigan State University
in partial fulfillment of the requirements
for the degree of

DOCTOR OF PHILOSOPHY

Applied Mathematics

2008

ABSTRACT

MATHEMATICAL ANALYSIS OF MULTICAPILLARY SUPPLY REGION

By

Liang Sun

This dissertation presents a mathematical analysis of substrate diffusion and consumption in a capillary-tissue bed. The model contains multiple non-homogeneous capillaries convecting different amount of solute surrounded by a tissue region. In the first section of this dissertation, solutions are obtained for a rectangular supply region where there are multiple capillaries. Both of its steady and transient states are completely analyzed. The time-wise evolution shows that hypoxia occurs during an early state and is restored as time increases. Furthermore, effect of axial diffusion in a 3-D model is analyzed in an extension where multicapillaries are embedded in a cylindrical tissue region. Perturbation method is employed to solve the associated governing equations. Finally, the dissertation introduces a numerical compartmental model for analyzing multicapillary free boundary supply regions. Hexagonal compartments are used to solve the diffusion-consumption governing equation.

Capillary-tissue domains are reported of three types of boundary: rectangular, circular and with free boundary. A matching technique is used to analytically solve the problem with regular domain boundary (i.e. rectangular or circular), in which the solution is expanded into an infinite eigenfunction form with unknown coefficients. The resulting equations inverted using Fourier series methods together with the Neumann boundary conditions are solved for the remaining unknown coefficients. Moreover, the time-dependent diffusion is investigated numerically and the solution to its equation is approximated by the Ficks law of diffusion. Hexagonal compartments are utilized for simple implementation.

ACKNOWLEDGMENT

I would like to express my gratitude to my thesis advisor, Professor C.Y. Wang, for bringing me into the world of Mathematical Biology, and for his guidance along this long journey. I would like to thank my parents, my brother and my sister in law, for their support and love. Without them I could not have reached this point and gone further. I am also thankful to the kind people and all my friends in East Lansing who have helped me and provided me the experiences that will benefit my life. I enjoyed every moment I spent there in the past few years.

TABLE OF CONTENTS

LIST OF TABLES

LIST OF FIGURES

Chapter 1

Introduction

Capillaries are tiny vessels connecting arterioles with venules and forming networks through the body. Oxygen diffusion from the microcirculation through capillaries and its consumption by tissue cells is basic in all higher organisms. A basic mathematical model to estimate the oxygen concentration profiles for highly regular capillary bed of skeletal muscle was originally introduced by Krogh [1]. Oxygen orientation is modeled by a central capillary surrounded by circular tissue cylinder. Extensions of the Krogh cylinder model have been made, including polygonal regions of supply, capillary effects, axial dependence, oxygen pressure etc.

Krogh cylinder among with many other models approximated oxygen distribution generated from homogeneous capillaries within regular capillary boundaries. Impermeable barriers and zero interactions among capillaries were also assumed. But in real cases, the capillaries may not be parallel, may be arranged more or less randomly in normal tissues. The oxygen concentration, along with its time-wise distribution, may be uneven. Therefore heterogeneity is considered much more common.

An important case of heterogeneity is abnormal perfusion. This may be caused by local ischemia due to blockage such as in heart attack, ischemic stroke, local collapse due to pressure and trauma. Where does such hypoxia occur? Would neighboring capillaries provide enough oxygen to the anoxic regions? How soon and how much?

These are the questions to be answered. Note again we are concerned about the scale of distance between capillaries and not global scale problems such as increase in demand due to exercise or reactive hyperemia after a tourquinet is released.

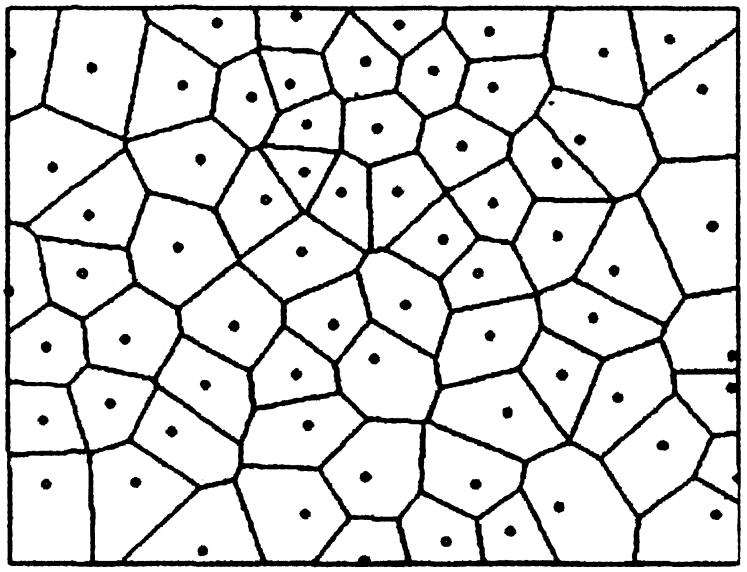

Figure 1.1: Multicapillaries in a tissue region where Voronoi boundaries are drawn

The last two cases mentioned above are primarily transient problems rather than heterogeneity problem. In transient problem time dependence is an essential factor and the effect is in global scale. For example, the observed periodicity in capillary flow rate is a transient problem if all capillaries are in phase and it is an heterogeneity problem if the capillaries are not in phase. As we shall see later the solution to a steady state heterogeneity problem may be sometimes obtained more easily through a transient process.

Consider a Long and parallel capillaries such as skeletal muscle. The time dependent development of anoxia can be simulated following occlusion in a multi-capillary domain with same (or different) diffusion solute. Some closer area to the capillary is more severely affected by such effect than the boundary area of the domain over a time interval. Remarkable advantage of application on diffusion equation is seen in such unsteady state, possessing its mathematical complexity and biological importance.

1.1 Krogh Model

Krogh[1] originally introduced the model for the study of oxygen distribution in the regular capillary beds of skeletal muscle. He used a perpendicular bisector to describe the oxygen transportation and concentration in tissues around blood capillaries. A hexagonal region was first considered. A circular region was addressed then for the boundary region assumedly only small error would occur if the hexagon is replaced by a disk. The steady state equation for the oxygen concentration in the tissue, $c(r, z, t)$ is then derived as following:

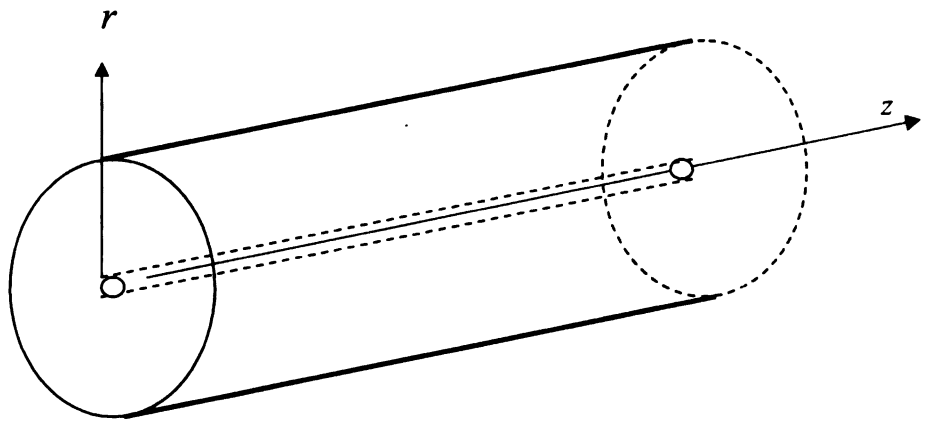

Figure 1.2: Geometry of the Krogh Cylinder: a single capillary surrounded by a coaxial cylinder of tissue

$$\frac{\partial c}{\partial t} = D_r \frac{1}{r}\frac{\partial}{\partial r}\left(r\frac{\partial c}{\partial r}\right) + D_z \frac{\partial^2 c}{\partial z^2} - M \tag{1.1}$$

Where D_r and D_z are the diffusion coefficients along the direction of r and z. M is the constant consumption rate per volume of tissue.

The longitudinal diffusion of oxygen can be neglected because the length of the cylinder is comparably 100 times longer than the radius of the cylinder. By considering only the steady state diffusion and neglecting the axial transportation among capillaries and in the tissue, the governing equation (1.1) then becomes a one dimen-

sional diffusion-consumption equation:

$$D_r \frac{1}{r}\frac{d}{dr}\left(r\frac{dc}{dr}\right) = M \tag{1.2}$$

with boundary conditions

$$c(r_c) = c_0 \tag{1.3}$$

$$\frac{dc}{dr}\,|_{r=r_t} = 0 \tag{1.4}$$

where r_c is the capillary radius and r_t gives the radius of the tissue cylinder.

Krogh gave a analytical solution under the simplified conditions:

1. Substrate concentrations were assumed to be in steady state
2. Axial movement was neglected:
3. The concentration is c_0 in the capillary.
4. No flux comes in or out of tissue cylinder

The solution to Eqs. (1.2) to (1.4) is the Krogh-erlang equation [1]:

$$c = c_0 - \left(\frac{M}{2D} r_t^2 ln\left(\frac{r}{r_c}\right) - \frac{r^2 - r_c^2}{2}\right) \tag{1.5}$$

As we see in the next few chapters, i) unsteady state is far more desirable especially in cases of hypoxia and anoxia. ii) a single capillary supply region could not be approximated in the multi-capillary domain, and multi-capillaries with arbitrary characteristics yield more complex results and the 1-D equation becomes a 2-D equation.

1.2 Capillary Supply Region and Capillary Domain

For multiple capillaries, the geometric area or volume allotted to each capillary is usually not the same as the capillary supply region. The former is called the capillary domain which is a descriptive measure of capillary spacing ([49], [60]). The latter is a

functional measure of the capillary diffusion region and would change with changes in perfusion, such as partial occlusion of some capillaries. Voronoi polygons are usually used to best describe capillary domains, which coincide with capillary supply regions if the capillaries are of the same strength and even distribution. Some special uneven periodic distributions are also possible(Fig 1.3).

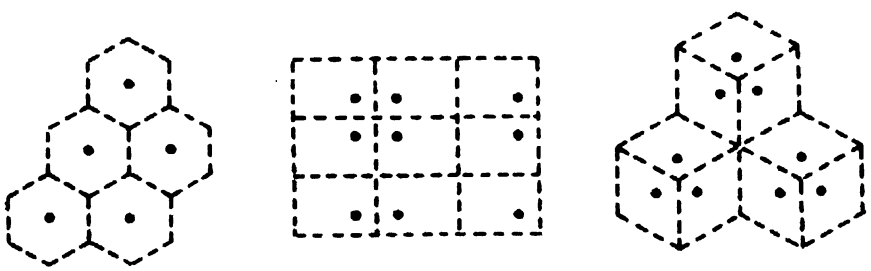

Figure 1.3: Some special cases of capillary supply boundaries which are also Voronoi boundaries

However, if the capillaries are of different characteristics, i.e. different location and strength, then Voronoi boundary could not be the capillary supply boundary. Consider two adjacent nodes of different source strength. The voronoi boundary is the perpendicular bisector(Fig 1.4(a)). But the concentration of the solute is not the same at the midpoint. Consequently the capillary supply boundary must shift toward the weaker node. It may also be curved as in Fig. 1.4(b).

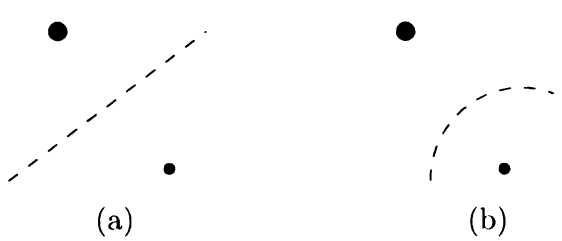

Figure 1.4: (a)Voronoi boundary, (b)capillary supply boundary. (Size of dot represents source strength)

Due to arbitrary characteristics of multicapillaries inside a micro piece of tissue, where the shape and the boundary of capillary supply region are highly related to the location and strength of its capillary, it is important to study such a feature which best describes the substrate diffusion.

1.3 Literature Review

Krogh first proposed the conceptual model to describe the oxygen distribution and exchange by substrate molecules from capillaries to tissue. This model was later known as Krogh cylinder which is presented in section 1.2. In Krogh's work, diffusion equation was used and simplified to obtain a analytical solution of concentration for oxygen inside a cylindrical skeleton tissue region. Since then considerable effort has been made to develop more a elaborate analysis of the model. Significant simplifications has been made to keep the mathematics tractable, resulted from the complex nature of the physiological phenomena.

Based on the Krogh cylinder, Jacob Blum [40], in 1960, presented a paper on the mathematical analysis of a model for substrate concentration in tissue in the American Journal of Physiology. His model analyzes the oxygen perfusion from a single capillary into its surrounding cylinder of tissue. Other works, for example, [20], [22], [38], [39] and [58] involved the effects of myoglobin, the effects of axial diffusion within tissue,on the single capillary model. Apelblat, Katzir-Katchalsky and Silberberg [2] gave a mathematical analysis of capillary-tissue fluid exchange in 1974. Most of the previous works have simplified the diffusion equation by neglecting the axial diffusion, which has relatively small effect compared to the radial diffusion. Mathematical analysis of oxygen transport to tissue which included axial diffusion within the tissue was studied by Salathe, Wang and Gross [24]. Their model used perturbation techniques to determine the axial diffusion effect for a single capillary in a Krogh cylinder. Fletcher [33], [34], [35] and Lih [52], reviewed several accounts

of mathematical studies of substrate and oxygen transport inside the Krogh cylinder. Significant simplifications has been made due to the complex nature of the governing equations. Numerical analysis in solving the full equations can also be found in works of Fletcher et. al. [33], [34], [35], Hyman [64] and Reneau et al [14], [15], [16].

In 1972, Gonzalez-Fernandez and Atta [42] numerically computed the non-circular equilateral triangular, square and hexagonal cylinders. It was found that the corners of the polygons are most susceptible to hypoxia (lethal corner). The stacking of regular polygonal cylinders still require both (1) all capillaries are same (flow, substrate diameter) and (2) capillaries are evenly distributed in a regular array. Schmidt-Nielsen and Pennycuik [46] discovered a triangular regional feature for white skeletal muscles with capillary-to-fiber ratio approximately equal to one. Opitz and Schneider [18] used a square region of supply for brain capillaries. These authors used polygonal region for capillary supply rather than a disk and estimated minimum tissue pressure within the supply region. But their target tissue contains only one single capillary and they assumed a uniform distribution of capillary locations across the whole tissue region. Such a case might exist in the real situation due to arbitrary capillary characteristics.

A single Krogh cylinder would represent all by symmetry. While single capillary models give useful information about oxygen exchange between tissue and capillary, they overlook the intensive large scale interactions among the many capillaries comprising a vascular bed. Capillaries, the microscopic size blood vessels, link the muscle with the cardiovascular system by a common arteriole and drained by a common venule. Each muscle cell may have from three to eight capillaries directly in contact with it. Blood flow along with substrate and oxygen distribution from capillaries to tissue through such a network of multi-vessels is critical. Therefore, the delivery of oxygen from the richly perfused to a poorly perfused region may definitely involve interactions among the neighboring capillaries. Thus studies the capillaries of different

strength and unevenly distributed throughout the tissue region are urgently needed to reflect the actual situation.

Numerical methods were used extensively to solve for multi-capillary models. A.S. Popel [8] studied the effect of multi-capillary network anastomoses an tortuosity on oxygen transport using computational methods to treat a reasonable sized array of capillaries, as well as some later work [6] he has done on heterogeneous oxygen delivery on oxygen distribution in skeletal muscle. In 1978, A.S. Popel published a paper in analysis of capillary tissue diffusion in multi-capillary systems. M.Sharan et al. [53] provided a finite-element analysis of oxygen transport in the systemic capillaries in 1991. All previous work faced the problem of requiring large amount of computation time and imposing restrictions on the number of capillaries that can be included. Salathe [18] used a homogenization approach to analyze a large number of capillaries in skeletal muscles, where capillaries are lined relatively long and parallel to each other. However, homogeneities are usually not the real case and heterogeneity is much more common.

Previous work which studied uneven capillaries include Clark et al. [55] who used a method of imaging. However, in his study capillary supply regions were not considered. Hoofd et al. [50] and Hoofd [48] required only the net flux on the boundary be zero. Diffusion within the planes perpendicular to the capillaries was determined using iterative method in Hoofd's study. However, without any control over the resulting boundary conditions the solution may be non-unique, therefore difficult to implement. R. Hsu and T.W. Secomb [57] used a green's function method for analysis of oxygen delivery to tissue by microvascular networks. It allows multi-capillaries with arbitrary characteristics within the tissue region, but becomes intractable when the integral equation is approximated by a system of algebraic equations. In 1999, Wang [12] studied capillary supply region for multiple capillaries (evenly or unevenly distributed) in a disk region and gave fully analytical solutions to the oxygen concen-

tration and discovered that the capillary supply region shapes substantially different from Krogh cylinder.

More recently, Salathe [19] presented a multi-capillary approach which includes exchange of substrates in a two dimensional array of capillaries. In his work, substrate concentration is determined in an rectangular or square tissue area consisting of a single capillary, where flux satisfies the outer boundary of the region as a result of interaction among all adjacent capillaries. By matching the substrate concentration along the boundaries, it provides a system of ordinary differential equations and can be solved analytically. Homogeneity is again assumed here.

The method described in chapter two in this thesis exploits a matching technique which solves the substrate diffusion within a rectangular tissue domain where multi-capillaries are unevenly or randomly distributed. Both steady state and unsteady state of the capillary supply are presented. In chapter three, axial diffusion is considered, treated as some perturbation to substrate concentration along the axial direction of multi capillaries. And in chapter four, a compartmental numerical model is introduced where hexagonal compartments are employed as functional units. Substrate diffuses along the borders of each compartment from the sources of substrate governed by Fick's diffusion law. Substrate concentration can then be approximated for unevenly distributed multi capillaries with free boundary domains.

Chapter 2

Multi-Capillary Supply within Rectangular Domains

Single capillary supply region has been modeled historically as in circular, hexagonal or polygonal regions. A uniform distribution of capillary locations across the whole tissue region was assumed and minimum tissue pressure within the supply region was estimated. However such case might not be suitable and is far from being complete when interactions among capillaries exist and multiple capillaries are considered. In this chapter, a mathematical analysis of the capillary-tissue exchange of substrate in microcirculation in rectangular regions when multiple capillaries are embedded with arbitrary characteristics will be presented. A matching technique is used to help solve the associated governing equations. Furthermore, the time-dependent unsteady state in a rectangular region will be modeled and examples will be illustrated. As we will see, sudden abolishment of steady state creates hypoxia area which is recovered and restored slowly during capillary-tissue substrate diffusion. Such a process is reversible if sufficient amount of substrate flux is convected through the capillaries.

2.1 Steady State of Multi-Capillary Supply in a Rectangular Region

This sections focus on oxygen concentration for multiple capillaries in a rectangular tissue region. We start with discussion of steady state. The ideal case is to have diffusion equation $\nabla^2 C = 1$ with no flux in or out of the boundary. The pinpoint results benefit from 1) Filing of circular regions leave voids in the tissue area and thus is not suitable to be extended to a greater tissue area. 2) in certain human functional capillaries like brain tissues, a region of square or rectangular is more suitable the case (Opitz and Schneider [18]). 3) it is easier to take account of unevenness, heterogeneity and flow variations of multi-capillaries when we study this supply region.

2.1.1 Formulation

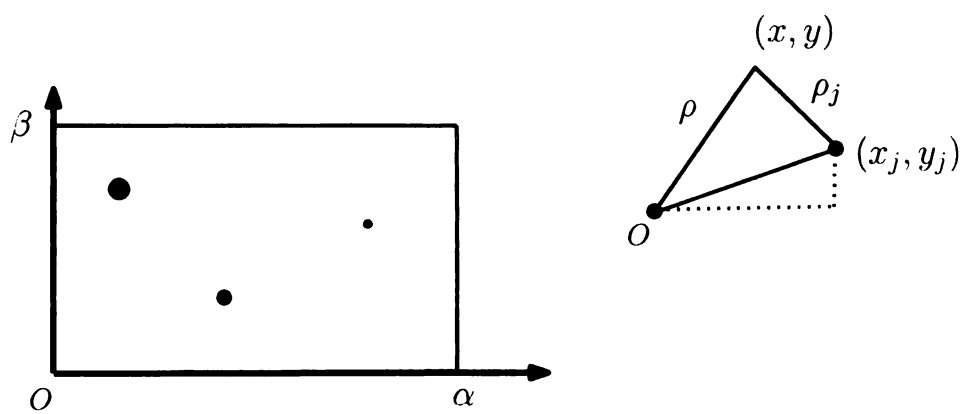

Figure 2.1: (a) A general distribution of capillaries in a rectangular region, (b) the coordinate system. O represents its origin of the Cartesian coordinates.

Consider a large rectangular region Ω of length α and width β, containing N capillaries of uneven locations and flux strength. We assume a uniform consumption rate κ per volume across Ω. Let q_j be the rate of oxygen perfusing into tissue area from the jth capillary source, with radius ρ_c centered at $x = x_j$, $y = y_j$. Considering

the steady state of the oxygen distribution, we have the mass flux balance which give s the condition on q_j

$$\sum_{j=1}^{N} q_j = \kappa \cdot \alpha \cdot \beta \tag{2.1}$$

The governing equation in two dimensional is given by diffusion equation:

$$D_r \nabla \cdot \nabla C(x,y) = \kappa, \quad C(x,y) \in \Omega \tag{2.2}$$

Where D_r is the diffusion coefficient of oxygen. On the boundary of the region there is no flux

$$\frac{\partial C}{\partial x}\Big|_{x \to 0,\alpha} = 0 \tag{2.3}$$

$$\frac{\partial C}{\partial y}\Big|_{y \to 0,\beta} = 0 \tag{2.4}$$

Let (ρ_j, φ_j) be local cylindrical coordinates centered at each capillary. Due to consistent flux into tissue area from capillary wall, the value of κ is zero. The equation for each capillary source is

$$D_p \left(\frac{\partial^2 c}{\partial \rho_j^2} + \frac{1}{\rho_j} \frac{\partial c}{\partial \rho_j} \right) = 0 \tag{2.5}$$

The boundary condition for each capillary is

$$q_j = -D_p \cdot \rho_r \int_0^{2\pi} \frac{\partial c}{\partial \rho_j}\Big|_{\rho_j \to \rho_r} d\varphi_j, \tag{2.6}$$

where D_p is the diffusion coefficient in capillary and ρ_r is the radius of capillary. Normalize the flux by $\alpha\beta$ and the diffusion by D_p, the equations for diffusion in capillaries are

$$\begin{cases} \dfrac{\partial^2 c}{\partial \rho_j^2} + \dfrac{1}{\rho_j}\dfrac{\partial c}{\partial \rho_j} = 0 \\ q_j = -\dfrac{\varepsilon}{\pi}\displaystyle\int_0^{2\pi} \dfrac{\partial c}{\partial \rho_j}\Big|_\varepsilon d\varphi_j, \quad \varepsilon = \dfrac{\rho_r}{R} \ll 1 \\ \displaystyle\sum_{j=1}^{N} q_j = 1. \end{cases} \tag{2.7}$$

Normalize the concentration in (2.2) by κ/D_T, the equation for oxygen diffusion in region Ω is

$$\Delta C(x,y) = 1, \quad C(x,y) \in \Omega \tag{2.8}$$

with boundary condition :

$$\begin{cases} q_j = -\dfrac{\varepsilon}{\pi}\displaystyle\int_0^{2\pi} \dfrac{\partial c}{\partial \rho_j}\Big|_\varepsilon d\varphi j \\ \dfrac{\partial C}{\partial x}\Big|_{x\to 0,\alpha} = 0, \quad \dfrac{\partial C}{\partial y}\Big|_{y\to 0,\beta} = 0 \end{cases} \tag{2.9}$$

2.1.2 Matching Technique and Scheme

Diffusion equation in a rectangular region Ω with Dirichlet or Neumann boundary condition has been studied and can be solved by using free Green functions and method of image. Notice boundary condition (2.9) is case specific due to a constant flux out of muti-capillaries at different locations, i.e singular points as $\epsilon \to 0$ within the region Ω, it's no longer a simple Neumann problem. Here we use a different strategy for solving Eqs (2.8) to assume general solution in the form

$$C(x,y) = (x^2 + y^2)/4 - \sum_{j=1}^{N} q_j/2 \cdot ln\rho_j + T(x,y) \tag{2.10}$$

The first term is a particular solution due to uniform consumption. The second term is the combination of fluxes from Eqs (2.7). The last term T is the homoge-

neous solution which is constructed in order to satisfy the boundary condition on the rectangular region Ω. To satisfy the boundary conditions with no substrate flowing across,we use the process of matching of boundary conditions and apply the series method to construct a suitable function $T(x, y)$.

Quote from Philip M Morse, Herman Feshbach (1953) *"The process of fitting of boundary conditions is somewhat analogous to the process of solving an ordinary differential equation. In neither case is the procedure straightforward; We must assume some general forms, which seems likely to satisfy our requirements, and then adjust things to satisfy them in detail (if, indeed, this turns out to be possible!) Many of our guesses for solutions of differential equations are very general in form such as power series or integral representations, but we find the specific solution by inserting the assumed form into the differential equation and then trying to make it fit."*

The boundary conditions are the particular Neumann conditions on a closed rectangular boundary. We separate our solution to satisfy the required boundary conditions on four walls along $x = 0$, $x = \alpha$, $y = 0$ and $y = \beta$. Consider, to begin with, that a series solution has flux zero along $x = \alpha$, $y = 0$ and $y = \beta$ and has an arbitrary sequence of values $\psi_s(x)$ (inhomogeneous conditions) along $x = 0$. After separation of variables from homogeneous equation associated with Eq. (2.8), the solution of the x equation which has derivative zero at $x = \alpha$ is $cosh\omega_\beta(x - \alpha)$, where n is integer and ω_β is the frequency representing $n\pi/\beta$, and the solution of the y equation which has derivative zero at $y = 0$ and $y = \beta$ is $\cos\omega_\beta y$.

Consequently the most general solution of $\nabla^2\psi = 0$, in two dimensions, which satisfies the homogeneous Neumann conditions that ψ has derivative zero along $x = \alpha$,

$y = 0$ and $y = \beta$ can be represented by the series

$$\psi = \sum_{n=0}^{\infty} A_n \cosh \omega_\beta (x - \alpha) \cos \omega_\beta y \tag{2.11}$$

The crucial step is to justify the functions in its above series form can satisfy all possible Neumann conditions along $x = 0$ and thus it can represent all possible solutions satisfying the zero-flux conditions along the three sides. Because we know Neumann conditions along a closed boundary specify a unique solution up to an additional constant. Then if we find another form of conditions, we can be sure that this new form corresonds to the series and, vice versa, that the series can represent the new form.

(Theorem 2.1) *A least squares representation of a piecewise continuous function $F(z)$ in Ω can be achieved if the sequence of eigenfunctions is a complete set. i.e. mutually orthogonal. And therefore the series form can represent general solution to the differential equation.*

$$\oint [\psi(z) - F(z)]^2 dx = 0$$

The eigenfunctions $\cos(n\pi y/\beta)$ as a factor in the partial solution (2.11) giving its dependence along the boundary surface depends on a separation constant as well as on position y along the boundary $x = 0$. This factor also satisfy the boundary conditions at the ends $y = 0$ and $y = \beta$. Here the constant are specially determined to fit the conditions at the chosen boundary sides. The other factor $\cosh [\frac{n\pi}{\beta}(x - \alpha)]$ is then adjusted to fit the conditions at the other end of the enclosed region Ω ($x = 0$ in our case), and the complete solution is then the sum of these products for all permissible values of the separation constant.

We have so far only considered the portion $x = 0$ of the boundary to have boundary values ψ to have boundary flux different from zero. To fit the conditions where ψ is different from zero along other parts of the rectangular boundary we can use obvious

modifications of the functions used in series (2.11). For instance, for fitting conditions along $y = 0$ we use the series

$$\sum_{n=0}^{\infty} D_n \cos\omega_\alpha x \ \cosh\omega_\alpha(y-\beta) \tag{2.12}$$

where $\omega_\alpha = n\pi/\alpha$. For $x = \alpha$ and $y = \beta$, adding the individual series to obtain the final solution. Therefore corresponding unit function can be derived here to fit the integrand for any boundary values at any point along the rectangular boundary. To solve the Eq.(2.8) and find the unit function in the series, we start with the choice of T for general solution to Eq. (2.8)

$$T = \psi_L + \psi_R + \psi_T + \psi_B \tag{2.13}$$

From previous discussion, the four terms can be seen as representation of general solutions against four boundary walls(left, right, top and bottom). Each term involves an unknown coefficient which is to be determined by combination of nonhomogeneous part of equation. And conveniently the four solution terms has property

$$\frac{\partial T}{\partial x}\Big|_{x\to 0} = \frac{\partial \psi_L}{\partial x}\Big|_{x\to 0}, \qquad \frac{\partial T}{\partial x}\Big|_{x\to \alpha} = \frac{\partial \psi_R}{\partial x}\Big|_{x\to \alpha} \tag{2.14}$$

$$\frac{\partial T}{\partial y}\Big|_{y\to \beta} = \frac{\partial \psi_T}{\partial y}\Big|_{y\to \beta}, \qquad \frac{\partial T}{\partial y}\Big|_{y\to 0} = \frac{\partial \psi_B}{\partial y}\Big|_{y\to 0} \tag{2.15}$$

2.1.3 Solution

The general form of T is

$$\begin{aligned} T = &\sum_{n=0}^{\infty} A_n \cosh\omega_\beta(x-\alpha) \ \cos\omega_\beta y + \sum_{n=0}^{\infty} B_n \cosh\omega_\beta x \ \cos\omega_\beta y \\ &+ \sum_{n=0}^{\infty} C_n \cos\omega_\alpha x \ \cosh\omega_\alpha y + \sum_{n=0}^{\infty} D_n \cos\omega_\alpha x \ \cosh\omega_\alpha(y-\beta) \end{aligned}$$

(2.16)

The relation between ρ_j, x_j, y_j is (Fig (2.1)(b))

$$\rho_j^2 = (x - x_j)^2 + (y - y_j)^2 \tag{2.17}$$

In order to determine the unknown coefficients A_n, B_n, C_n and D_n , we look at the boundary conditions given by (2.3) and (2.4). The oxygen concentration along each capillary walls depend on characteristics of capillary itself, therefore the radial outward normal at boundary $\bar{\Omega}$ of (2.10) gives

$$\frac{\partial C}{\partial x}\Big|_{x \to 0,\, \alpha} = \frac{x}{2} - \sum_{j=1}^{N} \frac{q_j}{4} \frac{2x - 2x_j}{(x - x_j)^2 + (y - y_j)^2} + \frac{\partial T}{\partial x} = 0 \tag{2.18}$$

and

$$\frac{\partial C}{\partial y}\Big|_{y \to 0,\, \beta} = \frac{y}{2} - \sum_{j=1}^{N} \frac{q_j}{2} \frac{y - y_j}{(x - x_j)^2 + (y - y_j)^2} + \frac{\partial T}{\partial y} = 0 \tag{2.19}$$

(2.16) gives

$$\begin{aligned} \frac{\partial T}{\partial x} = & \underbrace{\sum_{n=0}^{\infty} A_n \omega_\beta \sinh \omega_\beta (x - \alpha) \cos \omega_\beta y}_{I} + \underbrace{\sum_{n=0}^{\infty} B_n \omega_\beta \sinh \omega_\beta x \cos \omega_\beta y}_{II} \\ & \underbrace{- \sum_{n=0}^{\infty} C_n \omega_\alpha \sin \omega_\alpha x \cosh \omega_\alpha y}_{III} \underbrace{- \sum_{n=0}^{\infty} D_n \omega_\alpha \sin \omega_\alpha x \cosh \omega_\alpha (y - \beta)}_{IV} \end{aligned} \tag{2.20}$$

As $x \to 0$ the last three terms tend to approach zero, $II \to 0, III \to 0, IV \to 0$. therefore

$$\frac{\partial T}{\partial x}\Big|_{x\to 0} = \sum_{n=0}^{\infty} A_n \omega_\beta \sinh \omega_\beta(-\alpha)\, \cos \omega_\beta y = \frac{\partial \psi_L}{\partial x}\Big|_{x\to 0} \tag{2.21}$$

As $x \to \alpha$, $I \to 0, III \to 0, IV \to 0$

$$\frac{\partial T}{\partial x}\Big|_{x\to \alpha} = \sum_{n=0}^{\infty} B_n \omega_\beta \sinh \omega_\beta \alpha\, \cos \omega_\beta y = \frac{\partial \psi_R}{\partial x}\Big|_{x\to \alpha} \tag{2.22}$$

(2.21) and (2.22) gives the expression for zero flux flowing towards boundary $x \to 0$, α respectively, similarly for the vertical boundary lines $y \to 0$, β

$$\frac{\partial T}{\partial y} = \underbrace{\sum_{n=0}^{\infty} -A_n \omega_\beta (x-\alpha) \cosh \omega_\beta (x-\alpha)\, \sin \omega_\beta y}_{I} - \underbrace{\sum_{n=0}^{\infty} B_n \omega_\beta \cosh \omega_\beta x\, \sin \omega_\beta y}_{II}$$
$$+ \underbrace{\sum_{n=0}^{\infty} C_n \omega_\alpha \cos \omega_\alpha x\, \sinh \omega_\alpha y}_{III} + \underbrace{\sum_{n=0}^{\infty} D_n \omega_\alpha \cos \omega_\alpha x\, \sinh \omega_\alpha (y-\beta)}_{IV} \tag{2.23}$$

As $y \to 0$ $I \to 0, II \to 0, III \to 0$. therefore

$$\frac{\partial T}{\partial y}\Big|_{y\to 0} = \sum_{n=0}^{\infty} D_n \omega_\alpha \sinh \omega_\alpha(-\beta)\, \cos \omega_\alpha x = \frac{\partial \psi_T}{\partial y}\Big|_{y\to \beta} \tag{2.24}$$

As $y \to \beta$, $I \to 0, II \to 0, IV \to 0$

$$\frac{\partial T}{\partial y}\Big|_{y\to \beta} = \sum_{n=0}^{\infty} C_n \omega_\alpha \sinh \omega_\alpha \beta\, \cos \omega_\alpha x = \frac{\partial \psi_B}{\partial y}\Big|_{y\to 0} \tag{2.25}$$

Eqs. (2.21), (2.22),(2.24),(2.25) show that the form of solution (2.16) satisfies (2.14) and (2.15). It's then used to obtain the values for unknown coefficients A_n, B_n, C_n and D_n.

(Proposition 2.1) *Under (2.3) and (2.4), the general solutions to Eqs (2.8) with*

zero flux on boundary of the rectangular region bounded by $0 \le x \le \alpha$ *and* $0 \le y \le \beta$ *is*

$$C(x,y) = \frac{x^2+y^2}{4} - \sum_{j=1}^{N} \frac{q_j}{2} ln\rho_j + \sum_{n=0}^{\infty} \left[\begin{array}{l} A_n \cosh\left[\frac{n\pi}{\beta}(x-\alpha)\right] \cos\frac{n\pi y}{\beta} \\ + B_n \cosh\frac{n\pi}{\beta}x \cos\frac{n\pi y}{\beta} \\ + C_n \cos\frac{n\pi x}{\alpha} \cosh\frac{n\pi y}{\alpha} \\ + D_n \cos\frac{n\pi x}{\alpha} \cosh\left[\frac{n\pi}{\alpha}(y-\beta)\right] \end{array} \right] \tag{2.26}$$

Use the boundary conditions (2.18) and (2.21), as $x \to 0$

$$\frac{\partial C}{\partial x}\Big|_{x\to 0} = 0 + \sum_{j=1}^{N} \frac{q_j}{4} \frac{2x_j}{x_j^2+(y-y_j)^2} + \sum_{n=0}^{\infty} A_n \frac{n\pi}{\beta} \sinh\left[\frac{n\pi}{\beta}(-\alpha)\right] \cos\frac{n\pi y}{\beta} = 0 \tag{2.27}$$

$\Rightarrow$

$$\sum_{n=0}^{\infty} A_m \frac{n\pi}{\beta} \sinh\left[\frac{n\pi}{\beta}(-\alpha)\right] \cos\frac{n\pi y}{\beta} = \underbrace{\sum_{j=1}^{N} \frac{q_j}{2} \frac{-x_j}{x_j^2+(y-y_j)^2}}_{g_1(y)} \tag{2.28}$$

Multiply Eq.(2.28) by $\cos\frac{m\pi}{\beta}y$ and integrate from $-\beta$ to β with respect to y

$$A_m \frac{m\pi}{\beta} \sinh\left[\frac{m\pi}{\beta}(-\alpha)\right] \cdot \pi = \int_{-\beta}^{\beta} g_1(y) \cdot \cos\frac{m\pi}{\beta}y \, dy \tag{2.29}$$

Where $g_1(y) = \sum_{j=1}^{N} \frac{q_j}{2} \frac{-x_j}{x_j^2+(y-y_j)^2}$, Let $Y = (y-y_j)^2$, Eq.(2.24) yields

$$
\begin{aligned}
& A_m \frac{m\pi}{\beta} \sinh\left[\frac{m\pi}{\beta}(-\alpha)\right] \cdot \pi \\
&= \sum_{j=1}^{N} \frac{q_j}{2} \int_{-\beta}^{\beta} \frac{-x_j}{x_j^2 + (Y)^2} \left(\cos\frac{m\pi}{\beta} Y \cos\frac{m\pi}{\beta} y_j - \sin\frac{m\pi}{\beta} Y \sin\frac{m\pi}{\beta} y_j \right) dY \\
&= \sum_{j=1}^{N} \frac{q_j}{2} \int_{-\beta}^{\beta} \frac{-x_j}{x_j^2 + (Y)^2} \cos\frac{m\pi}{\beta} Y \cos\frac{m\pi}{\beta} y_j \, dY \\
&= \sum_{j=1}^{N} \frac{q_j}{2} (-x_j) \, 2 \cos\frac{m\pi}{\beta} y_j \int_0^{\beta} \frac{1}{x_j^2 + (Y)^2} \cos\frac{m\pi}{\beta} Y \, dY
\end{aligned}
\tag{2.30}
$$

Thus

$$
A_m = \frac{1}{m\pi \sinh\frac{m\pi}{\beta}(-\alpha)} \sum_{j=1}^{N} q_j \, (-x_j) \cos\frac{m\pi}{\beta} y_j \int_0^{\pi} \frac{1}{\frac{\pi^2}{\beta^2} x_j^2 + (y)^2} \cdot \cos my \, dy \tag{2.31}
$$

Here $y = \frac{m\pi}{\beta} Y$, and again (x_j, y_j) gives the location of the jth source. Similarly, we achieve the values for the unknown coefficients B_m, C_m and D_m

$$
B_m = \frac{1}{m\pi \sinh\frac{m\pi}{\beta}(\alpha)} \sum_{j=1}^{N} q_j \, (\alpha - x_j) \cos\frac{m\pi}{\beta} y_j \int_0^{\pi} \frac{\cos my}{\frac{\pi^2}{\beta^2}(\alpha - x_j)^2 + (y)^2} \, dy \tag{2.32}
$$

$$
C_m = \frac{1}{m\pi \sinh\frac{m\pi}{\alpha}(\beta)} \sum_{j=1}^{N} q_j \, (\beta - y_j) \cos\frac{m\pi}{\alpha} x_j \int_0^{\pi} \frac{\cos mx}{(x)^2 + \frac{\pi^2}{\alpha^2} y_j^2} \, dx \tag{2.33}
$$

$$
D_m = \frac{1}{m\pi \sinh\frac{m\pi}{\alpha}(-\beta)} \sum_{j=1}^{N} q_j \, (-y_j) \cos\frac{m\pi}{\alpha} x_j \int_0^{\pi} \frac{\cos mx}{(x)^2 + \frac{\pi^2}{\alpha^2}(\beta - y_j)^2} \, dx \tag{2.34}
$$

2.1.4 Examples and Discussion

Oxygen delivery to tissue has been studied in various ways. Many researches were limited to a single capillary. Popel [7] used evenly distributed domains for multi-capillaries with heterogeneous flow. However, with different oxygen demands multi-capillary supply region can not be approximated by single capillary capillary supply regions. Circular region has been studied by Wang [12] and analytical solutions was given. However, tiled circular regions will leave voids in tissue area and therefore can not represent the entire tissue region. However, rectangular regions can be tiled without voids into sub rectangular tissue regions. Thus we have used a matching technique to achieve complete solutions for oxygen concentration through a rectangular region. Three examples will be illustrated in the following

I. A single capillary in a well oxygenated diffusion-consumption rectangular region with $\alpha = 1$ and $\beta = 1$.

Consider a single capillary in the center of the region with flux strength $q = 1$. The results for coefficients are displayed in Table (2.1) to show the convergence of the series to the entire rectangular region. We also show the plot of oxygen concentration $C(x, y)$ in Fig. (2.2). We have truncated to only the first 40 terms in each set of coefficients. It reaches our accuracy demand.

	$n = 1$	$n = 2$	$n = 10$	$n = 20$	$n = 30$
A_n	-0.1019	-0.1006	1.066×10^{-5}	-1.796×10^{-6}	-3.001×10^{-9}
B_n	-0.1024	-0.1023	1.080×10^{-5}	-1.659×10^{-6}	-3.025×10^{-8}
C_n	-0.1024	-0.1023	1.080×10^{-5}	-1.659×10^{-6}	-3.025×10^{-8}
D_n	-0.1019	-0.1006	1.066×10^{-5}	-1.796×10^{-6}	-3.001×10^{-9}

Table 2.1: Coefficients of Example 1 for a rectangular domain up to $n = 30$ with $\alpha = 1$ and $\beta = 1$

II. Three random single capillaries in a well supplied diffusion-consumption rect-

angular region with $\alpha = 1$ and $\beta = 1$.

Consider three capillary of uneven strength in a rectangular region. Locations and flux strengths of the capillaries shown in table (2.2) are randomly generated with the sum of flux equal to 1. The results for coefficients are shown in Table (2.3) to show the convergence of the solution to the entire rectangular region. We also show the plot of oxygen concentration $C(x, y)$ in Fig. (2.3). We have truncated to only the first 40 terms in each set of coefficients since it reaches our accuracy goal.

k	x_k	y_k	q_k
1	0.721	0.637	0.176
2	0.812	0.243	0.412
3	0.175	0.320	0.412

Table 2.2: Locations and flux strengths of three capillaries in Example 2

	$n = 1$	$n = 2$	$n = 10$	$n = 20$	$n = 30$
A_n	0.0035	−0.0003	-1.160×10^{-6}	-1.310×10^{-8}	1.227×10^{-10}
B_n	0.0037	−0.0006	-5.216×10^{-7}	-1.804×10^{-8}	-3.078×10^{-10}
C_n	−0.6731	−0.0012	8.478×10^{-5}	-5.249×10^{-8}	4.606×10^{-9}
D_n	−0.0011	0.0003	1.153×10^{-7}	-7.940×10^{-9}	1.049×10^{-10}

Table 2.3: Coefficients of Example 2 for a rectangular domain up to $n = 30$ with $\alpha = 1$ and $\beta = 1$

III. Nine random single capillaries in a well sufficed diffusion-consumption rectangular region with $\alpha = 1$ and $\beta = 1$ with plot of contour.

Consider nine capillary of uneven strength in a rectangular region. Locations and flux strengths of the capillaries are randomly generated shown in table (2.4) with the sum of flux equal to 1. The results for coefficients are given in Table (2.5) and (2.6) to show the convergence of the solution to the entire rectangular region. We also show the plot of oxygen concentration level curve in Fig. (2.4). We have truncated to only the first 40 terms in each set of coefficients.

k	x_k	y_k	q_k
1	0.501	0.498	0.044
2	0.721	0.235	0.089
3	0.242	0.754	0.133
4	0.091	0.046	0.133
5	0.633	0.923	0.089
6	0.867	0.354	0.023
7	0.425	0.301	0.133
8	0.664	0.316	0.178
9	0.723	0.833	0.178

Table 2.4: Locations and flux strengths of nine capillaries in Example 3

	$n = 1$	$n = 2$	$n = 10$	$n = 20$	$n = 30$
A_n	-0.2884	0.0065	1.534×10^{-4}	2.615×10^{-6}	8.110×10^{-8}
B_n	-0.4366	0.0060	-5.671×10^{-4}	-6.174×10^{-6}	1.099×10^{-7}
C_n	-0.2591	-0.0047	1.790×10^{-4}	-2.513×10^{-6}	-6.557×10^{-8}
D_n	0.2254	0.0049	1.906×10^{-4}	2.441×10^{-6}	3.121×10^{-8}

Table 2.5: Coefficients of Example 3 for a rectangular domain up to $n = 30$ with $\alpha = 1$ and $\beta = 1$.

	$n = 40$	$n = 50$	$n = 60$
A_n	1.690×10^{-12}	3.871×10^{-14}	8.775×10^{-16}
B_n	8.553×10^{-14}	3.693×10^{-15}	1.263×10^{-16}
C_n	2.184×10^{-12}	-8.853×10^{-16}	-1.608×10^{-15}
D_n	-8.142×10^{-13}	-8.648×10^{-14}	4.239×10^{-15}

Table 2.6: Coefficients of Example 3 for a rectangular domain up from $n = 40$ to $n = 60$ with $\alpha = 1$ and $\beta = 1$.

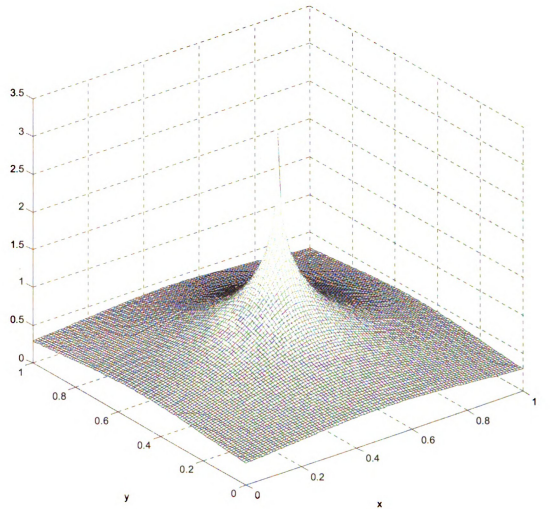

Figure 2.2: Oxygen concentration in its steady state with one single capillary inside a sufficiently oxygenated rectangular domain, $\alpha = 1$ and $\beta = 1$ Example 1.

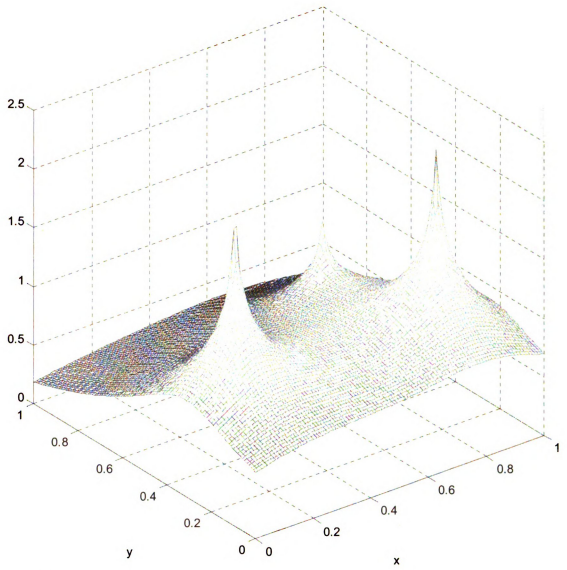

Figure 2.3: Oxygen concentration in its steady state with three capillaries inside a sufficiently oxygenated rectangular domain, $\alpha = 1$ and $\beta = 1$ Example 2.

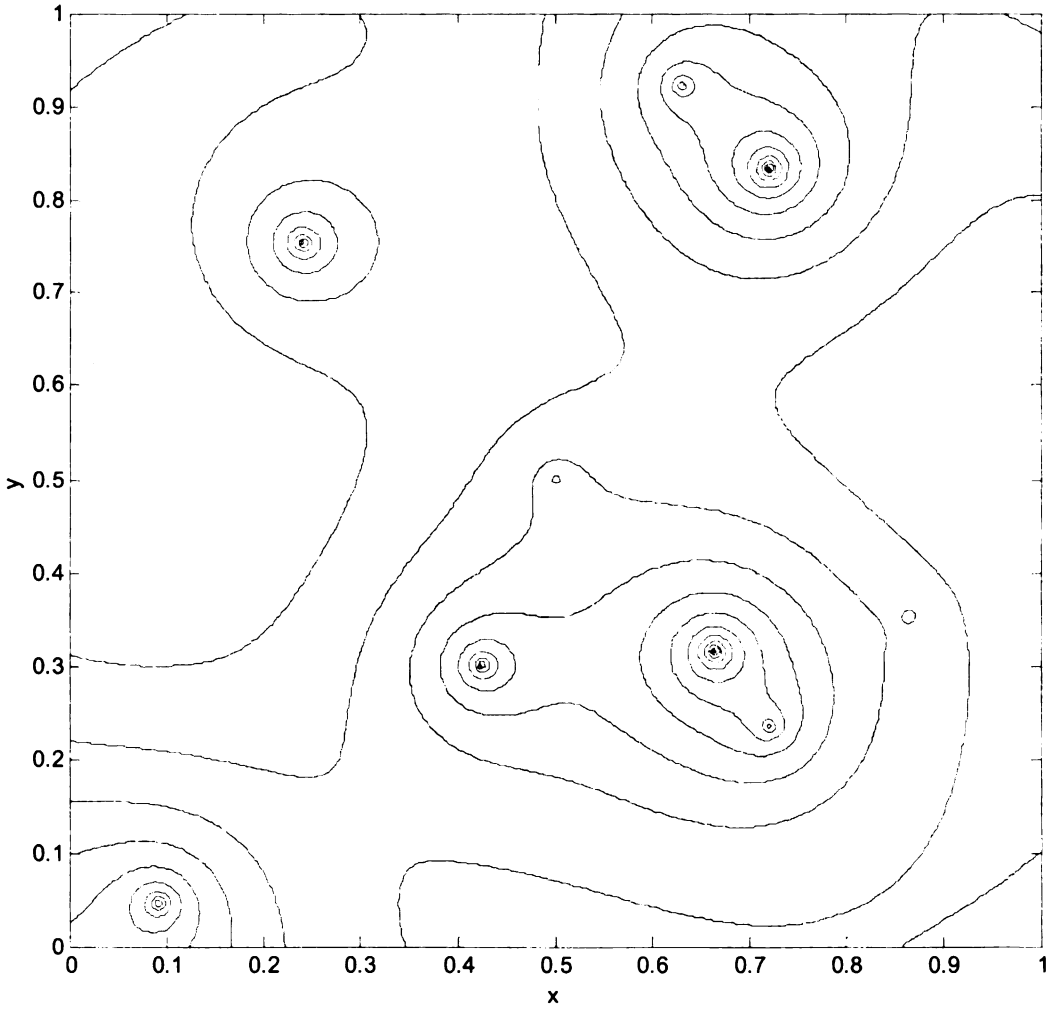

Figure 2.4: Oxygen concentration level curve in a sufficiently oxygenated rectangular domain with nine capillaries, steady state, $\alpha = 1$ and $\beta = 1$ Example 3.

2.2 Transient State of Multi-Capillary Supply in a Rectangular Region

Study of transient state of the oxygen distribution in tissue area is crucial and even more important than learning the steady state of such concentration. Since in the beginning the tissue cells might consume more oxygen than necessary, it helps to see the change of hypoxic area as time increases. And sometimes a lethal corner may exist and time dependent diffusion has this outstanding advantage to discover this instinct phenomenon.

2.2.1 Formulation and Solutions

Now let us consider again the rectangular tissue region Ω of length α and width β, containing N capillaries of uneven locations and flux strength. We may neglect the longitudinal diffusion of solute and derive the governing equation conveying oxygen from capillaries to tissue, after normalization of concentration by κ/D_T

$$\frac{\partial C}{\partial t} = \nabla^2 C - 1 \tag{2.35}$$

and boundary condition is

$$\begin{cases} q_j = -\dfrac{\varepsilon}{\pi}\displaystyle\int_0^{2\pi} \frac{\partial C}{\partial \rho_j}|_{\varepsilon} d\varphi_j \\ \dfrac{\partial C}{\partial x}\Big|_{x\to 0,\alpha} = 0, \quad \dfrac{\partial C}{\partial y}\Big|_{y\to 0,\beta} = 0 \end{cases} \tag{2.36}$$

To set up a strategy for solving this equation over a rectangular closed boundary with multiple source points, we first consider the homogeneous solution and treat the time dependence using the method of separation variables

$$C(x, y, t) = T(t)Q(x, y) \tag{2.37}$$

then for some unknown constant λ, we have

$$\frac{1}{T}T' = -\lambda \quad (2.38) \qquad \text{and} \qquad \Delta Q + \lambda Q = 0 \quad (2.39)$$

The solutions of the Eqs.(2.38) is

$$T = Ae^{-\lambda t} \tag{2.40}$$

The solution of T is exponentially decreasing along time. Without adding or subtracting a constant distribution $C_0(x, y)$, our initial condition here (when $t = 0$) is always the steady state of oxygen concentration. This complies the real case because 1. the consumption rate κ across the tissue area is never zero, and 2. the process of regaining steady state is important in biological metabolism. If necessary, we can subtract the steady state from the solution and add a constant C_0 as required from the initial substrate distribution in the rectangular tissue area.

The Eq (2.39) is a Helmholtz equation in two variables, with rectangular supports. We can set the solution by

$$Q = \sum_{n=0}^{\infty} \left[\begin{array}{l} A_n \cos\left[\sqrt{\lambda - \frac{n^2\pi^2}{\beta^2}}(x - \alpha)\right] \cos\frac{n\pi y}{\beta} \\ + B_n \cos\sqrt{\lambda - \frac{n^2\pi^2}{\beta^2}}x \cos\frac{n\pi y}{\beta} \\ + C_n \cos\frac{n\pi x}{\alpha} \cos\sqrt{\lambda - \frac{n^2\pi^2}{\alpha^2}}y \\ + D_n \cos\frac{n\pi x}{\alpha} \cos\left[\sqrt{\lambda - \frac{n^2\pi^2}{\alpha^2}}(y - \beta)\right] \end{array} \right] \tag{2.41}$$

where A_n, B_n, C_n and D_n are unknown constants bounded by the boundary

condition (2.36). Let $\delta(\hbar) = \sqrt{\lambda - \frac{n^2\pi^2}{\hbar^2}}$ Then the homogeneous solution is

$$C_h(t,x,y) = \int_0^\infty e^{-\lambda t} \sum_{n=0}^{\infty} \Big(A_n \cos\Big[\delta(\beta)(x-\alpha)\Big] \cos\frac{n\pi y}{\beta} + B_n \cos\delta(\beta)x \cos\frac{n\pi y}{\beta} + C_n \cos\frac{n\pi x}{\alpha} \cos\delta(\alpha)y + D_n \cos\frac{n\pi x}{\alpha} \cos\Big[\delta(\alpha)(y-\beta)\Big]\Big) d\lambda \tag{2.42}$$

To find the particular solution to Eq. (2.35), we can use a transform into $C_p = v + C_{ps}$, which provides

$$\frac{\partial v}{\partial t} = \nabla^2 v + \nabla^2 C_{ps} - 1 = \nabla^2 v \tag{2.43}$$

The C_{ps} is the particular solution in steady state and C_p is the particular solution in our modeling. Then the particular solution is thus

$$C_p(t,x,y) = \int_0^\infty e^{-\lambda t} \sum_{n=0}^{\infty} \Big(E_n \cos\Big[\delta(\beta)(x-\alpha)\Big] \cos\frac{n\pi y}{\beta} + F_n \cos\delta(\beta)x \cos\frac{n\pi y}{\beta} + G_n \cos\frac{n\pi x}{\alpha} \cos\delta(\alpha)y + H_n \cos\frac{n\pi x}{\alpha} \cos\Big[\delta(\alpha)(y-\beta)\Big]\Big) d\lambda + \frac{x^2+y^2}{4} \tag{2.44}$$

The source solution of j th capillary (2.7) and the Eq. (2.17) together with the homogeneous solution (2.42) and particular solution (2.44) yield to the general solution of oxygen diffusion

$$C(t,x,y) = \frac{x^2+y^2}{4} + G - \sum_{j=1}^{N} \frac{q_j}{4} ln\Big[(x-x_j)^2 + (y-y_j)^2\Big] \tag{2.45}$$

where

$$G = \int_0^\infty e^{-\lambda t} \sum_{n=0}^{\infty} \Big(\bar{A}_n \cos \Big[\delta(\beta)(x-\alpha)\Big] \cos \frac{n\pi y}{\beta} + \bar{B}_n \cos\, \delta(\beta)x\, \cos \frac{n\pi y}{\beta} + \bar{C}_n \cos \frac{n\pi x}{\alpha}\, \cos\, \delta(\alpha)y + \bar{D}_n \cos \frac{n\pi x}{\alpha} \cos \Big[\delta(\alpha)(y-\beta)\Big] \Big)\, d\lambda \qquad (2.46)$$

In the Eq. (2.45), the first term is particular solution due to uniform consumption. The second term is homogeneous solution and third term is the combination of sources from each capillary. Being still more specific, we can compute the required values of the coefficients $\bar{A}_n, \bar{B}_n, \bar{C}_n$ and $\bar{D}_n$ by using the boundary conditions at the four rectangular walls

$$\frac{\partial C}{\partial x}\Big|_{x \to 0,\, \alpha} = \frac{x}{2} - \sum_{j=1}^{N} \frac{q_j}{4} \frac{2x - 2x_j}{(x-x_j)^2 + (y-y_j)^2} + \frac{\partial G}{\partial x} = 0 \qquad (2.47)$$

and

$$\frac{\partial C}{\partial y}\Big|_{y \to 0,\, \beta} = \frac{y}{2} - \sum_{j=1}^{N} \frac{q_j}{2} \frac{y - y_j}{(x-x_j)^2 + (y-y_j)^2} + \frac{\partial G}{\partial y} = 0 \qquad (2.48)$$

(2.46) gives

$$\frac{\partial G}{\partial x} = \int_0^\infty e^{-\lambda t} \Bigg(\underbrace{- \sum_{n=0}^{\infty} \bar{A}_n \delta(\beta) \sin\, [\delta(\beta)(x-\alpha)] \cos \frac{n\pi y}{\beta}}_{I} \underbrace{- \sum_{n=0}^{\infty} \bar{B}_n \delta(\beta) \sin\, \delta(\beta)x\, \cos \frac{n\pi y}{\beta}}_{II} \underbrace{- \sum_{n=0}^{\infty} \bar{C}_n \frac{n\pi}{\alpha} \sin \frac{n\pi x}{\alpha} \cos \delta(\alpha)y}_{III} \underbrace{- \sum_{n=0}^{\infty} \bar{D}_n \frac{n\pi}{\alpha} \sin \frac{n\pi x}{\alpha} \cos[\delta(\alpha)(y-\beta)]}_{IV} \Bigg) d\lambda \qquad (2.49)$$

As $x \to 0$ the last three terms tend to approach zero, $II \to 0, III \to 0, IV \to 0$. therefore

$$\left.\frac{\partial G}{\partial x}\right|_{x\to 0} = \int_0^\infty e^{-\lambda t} \sum_{n=0}^{\infty} \bar{A}_n \delta(\beta) \sin\left[\delta(\beta)\alpha\right] \cos\frac{n\pi y}{\beta}\, d\lambda \tag{2.50}$$

As $x \to \alpha$, $I \to 0, III \to 0, IV \to 0$

$$\left.\frac{\partial G}{\partial x}\right|_{x\to \alpha} = -\int_0^\infty e^{-\lambda t} \sum_{n=0}^{\infty} \bar{B}_n \delta(\beta) \sin\ \delta(\beta)x\ \cos\frac{n\pi y}{\beta}\, d\lambda \tag{2.51}$$

Similarly for the vertical boundary lines $y \to 0,\ \beta$

$$\begin{aligned}\frac{\partial G}{\partial y} = \int_0^\infty e^{-\lambda t}\Bigg(&\underbrace{-\sum_{n=0}^{\infty} \bar{A}_n \frac{n\pi}{\beta} \cos\left[\delta(\beta)(x-\alpha)\right] \sin\frac{n\pi y}{\beta}}_{I} \\ &\underbrace{-\sum_{n=0}^{\infty} \bar{B}_n \frac{n\pi}{\beta} \cos\ \delta(\beta)x\ \sin\frac{n\pi y}{\beta}}_{II} \\ &\underbrace{-\sum_{n=0}^{\infty} \bar{C}_n\, \delta(\alpha) \cos\frac{n\pi x}{\alpha} \sin\delta(\alpha)y}_{III} \underbrace{-\sum_{n=0}^{\infty} \bar{D}_n \delta(\alpha) \cos\frac{n\pi x}{\alpha} \sin[\delta(\alpha)(y-\beta)]}_{IV}\Bigg)\, d\lambda\end{aligned} \tag{2.52}$$

As $y \to 0$ $I \to 0, II \to 0, III \to 0$. therefore

$$\left.\frac{\partial T}{\partial y}\right|_{y\to 0} = \int_0^\infty e^{-\lambda t} \sum_{n=0}^{\infty} \bar{D}_n \delta(\alpha) \cos\frac{n\pi x}{\alpha} \sin\left[\delta(\alpha)\beta\right] d\lambda \tag{2.53}$$

As $y \to \beta$, $I \to 0, II \to 0, IV \to 0$

$$\left.\frac{\partial T}{\partial y}\right|_{y\to\beta} = -\int_0^\infty e^{-\lambda t} \sum_{n=0}^{\infty} \bar{C}_n \delta(\alpha) \cos\frac{n\pi x}{\alpha} \sin\ \delta(\alpha)\beta\, d\lambda \qquad (2.54)$$

Eqs(2.47) and (2.50) yield

As $x \to 0$

$$\left.\frac{\partial C}{\partial x}\right|_{x\to 0} = 0 + \sum_{j=1}^{N} \frac{q_j}{4} \frac{2x_j}{x_j^2 + (y-y_j)^2} + \int_0^\infty e^{-\lambda t} \sum_{n=0}^{\infty} \bar{A}_n \delta(\beta) \sin\left[\delta(\beta)\alpha\right] \cos\frac{n\pi y}{\beta}\, d\lambda = 0 \qquad (2.55)$$

$\Rightarrow$

$$\int_0^\infty e^{-\lambda t} \sum_{n=0}^{\infty} \bar{A}_n\, \delta(\beta) \sin\ \delta(\beta)\,\alpha \cos\frac{n\pi y}{\beta}\, d\lambda = \sum_{j=1}^{N} \frac{q_j}{2} \frac{-x_j}{x_j^2 + (y-y_j)^2} \qquad (2.56)$$

Multiply Eq.(2.56) by $\cos\frac{m\pi}{\beta}y$ and integrate from $-\beta$ to β with respect to y

$$\bar{A}_m\, \pi \int_0^\infty e^{-\lambda t} \sum_{n=0}^{\infty} \delta(\beta) \sin\ \delta(\beta)\,\alpha\, d\lambda = \int_{-\beta}^{\beta} g_1(y) \cdot \cos\frac{m\pi}{\beta} y\, dy \qquad (2.57)$$

Let $Y = (y - y_j)^2$

$$
\begin{aligned}
&\bar{A}_m \pi \int_0^\infty e^{-\lambda t} \sqrt{\lambda - \frac{n^2\pi^2}{\beta^2}} \sin \sqrt{\lambda - \frac{n^2\pi^2}{\beta^2}}\, \alpha\, d\lambda \\
&= \sum_{j=1}^{N} \frac{q_j}{2} \int_{-\beta}^{\beta} \frac{-x_j}{x_j^2 + (Y)^2} \left(\cos\frac{m\pi}{\beta} Y \cos\frac{m\pi}{\beta} y_j - \sin\frac{m\pi}{\beta} Y \sin\frac{m\pi}{\beta} y_j \right) dY \\
&= \sum_{j=1}^{N} \frac{q_j}{2} \int_{-\beta}^{\beta} \frac{-x_j}{x_j^2 + (Y)^2} \cos\frac{m\pi}{\beta} Y \cos\frac{m\pi}{\beta} y_j\, dY \\
&= \sum_{j=1}^{N} \frac{q_j}{2} (-x_j)\, 2 \cos\frac{m\pi}{\beta} y_j \int_0^{\beta} \frac{1}{x_j^2 + (Y)^2} \cos\frac{m\pi}{\beta} Y\, dY
\end{aligned}
\tag{2.58}
$$

Thus

$$
\bar{A}_m = \frac{\sum_{j=1}^{N} q_j\, (-x_j) \cos\frac{m\pi}{\beta} y_j}{\beta \int_0^\infty e^{-\lambda t} \sqrt{\lambda - \frac{n^2\pi^2}{\beta^2}} \sin \sqrt{\lambda - \frac{n^2\pi^2}{\beta^2}}\, \alpha\, d\lambda} \int_0^\pi \frac{\cos my}{\frac{\pi^2}{\beta^2} x_j^2 + (y)^2} dy \tag{2.59}
$$

Here $y = \frac{m\pi}{\beta} Y$, and (x_j, y_j) is the location of the jth source. Similarly, the values for the unknown coefficients B_m, C_m and D_m are achieved

$$
\bar{B}_m = \frac{\sum_{j=1}^{N} q_j\, (\alpha - x_j) \cos\frac{m\pi}{\beta} y_j}{-\beta \int_0^\infty e^{-\lambda t} \sqrt{\lambda - \frac{n^2\pi^2}{\beta^2}} \sin \sqrt{\lambda - \frac{n^2\pi^2}{\beta^2}}\, \alpha\, d\lambda} \int_0^\pi \frac{\cos my}{\frac{\pi^2}{\beta^2} (\alpha - x_j)^2 + (y)^2} dy \tag{2.60}
$$

$$
\bar{C}_m = \frac{\sum_{j=1}^{N} q_j\, (-y_j) \cos\frac{m\pi}{\alpha} x_j}{\alpha \int_0^\infty e^{-\lambda t} \sqrt{\lambda - \frac{n^2\pi^2}{\alpha^2}} \sin \sqrt{\lambda - \frac{n^2\pi^2}{\alpha^2}}\, \beta\, d\lambda} \int_0^\pi \frac{\cos mx}{(x)^2 + \frac{\pi^2}{\alpha^2} y_j^2} dx \tag{2.61}
$$

$$
\bar{D}_m = \frac{\sum_{j=1}^{N} q_j\, (\beta - y_j) \cos\frac{m\pi}{\alpha} x_j}{-\alpha \int_0^\infty e^{-\lambda t} \sqrt{\lambda - \frac{n^2\pi^2}{\alpha^2}} \sin \sqrt{\lambda - \frac{n^2\pi^2}{\alpha^2}}\, \beta\, d\lambda} \int_0^\pi \frac{\cos mx}{(x)^2 + \frac{\pi^2}{\alpha^2} (\beta - y_j)^2} dx \tag{2.62}
$$

2.2.2 Analysis and Example

Oxygen diffusion from capillary supply in its transient state has rarely been studied. Many authors have treated the problem as in its steady state with highly simplified profiles. A steady state is always achieved through solving its time-independent equations. However in practice, during oxygen transport, substrates are perfused constantly along with the time. Some of the tissue may never achieve its steady state due to constant change of flux strength or sudden occlusion of capillaries. For example, some tissues suffer from sudden lack of oxygen during physical exertion. The hypoxia appears and the consumption rate rises even though the amount of oxygen out of each capillary preserves the initial quantity. It is common to all creature metabolism and therefore important to study the time-dependent oxygen transport. To illustrate the results we get from above sections, we use the following example with again $\alpha = 1$ and $\beta = 1$.

k	x_k	y_k	q_k
1	0.721	0.637	0.176
2	0.812	0.243	0.412
3	0.175	0.320	0.412

Table 2.7: Locations and flux strengths of three capillaries

Consider a rectangular region with three capillaries. The location and solute amount of each capillary are shown in table (2.7). We also plot the oxygen concentration level curves at $t = 0$, $t = 1$ and $t = 10$ as shown in Fig (2.5), (2.6) and (2.7).

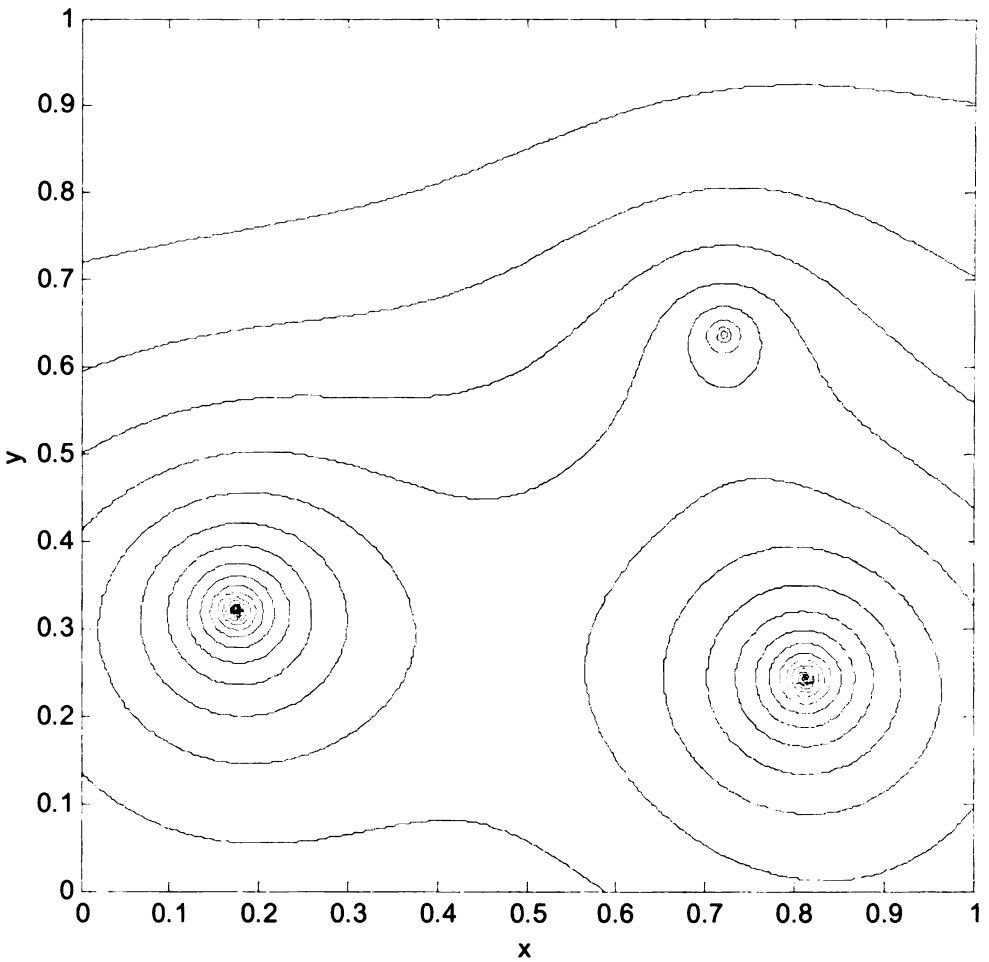

Figure 2.5: Oxygen concentration level curve at $t = 0$, transient state, three capillaries with random characteristics

Fig. (2.5) displays the oxygen concentration level at $t = 0$ for its steady state. At time $t = 1$, we can see from the Fig. (2.6) that hypoxia area occurs at the upper left region where consumption rate increases and less oxygen is supplied to this area. Fig. (2.7) shows that the hypoxia area is restored and moves slowly to the top y boundary. The hypoxia area is recovered as time increases. This might be due to the reason that the cells are very susceptible to the change of circumstance before they get used to new environment. And they may consume more oxygen than necessary in the beginning state. (Go [27])

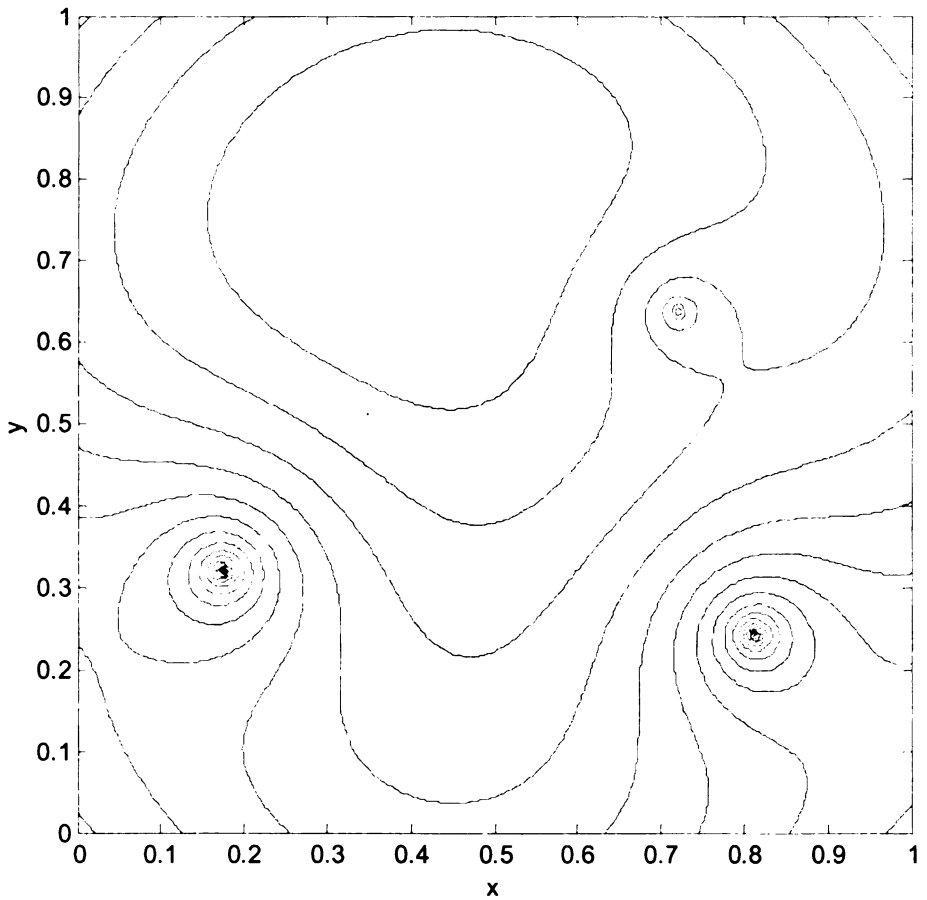

Figure 2.6: Oxygen concentration level curve at $t = 1$, transient state, three capillaries with random characteristics

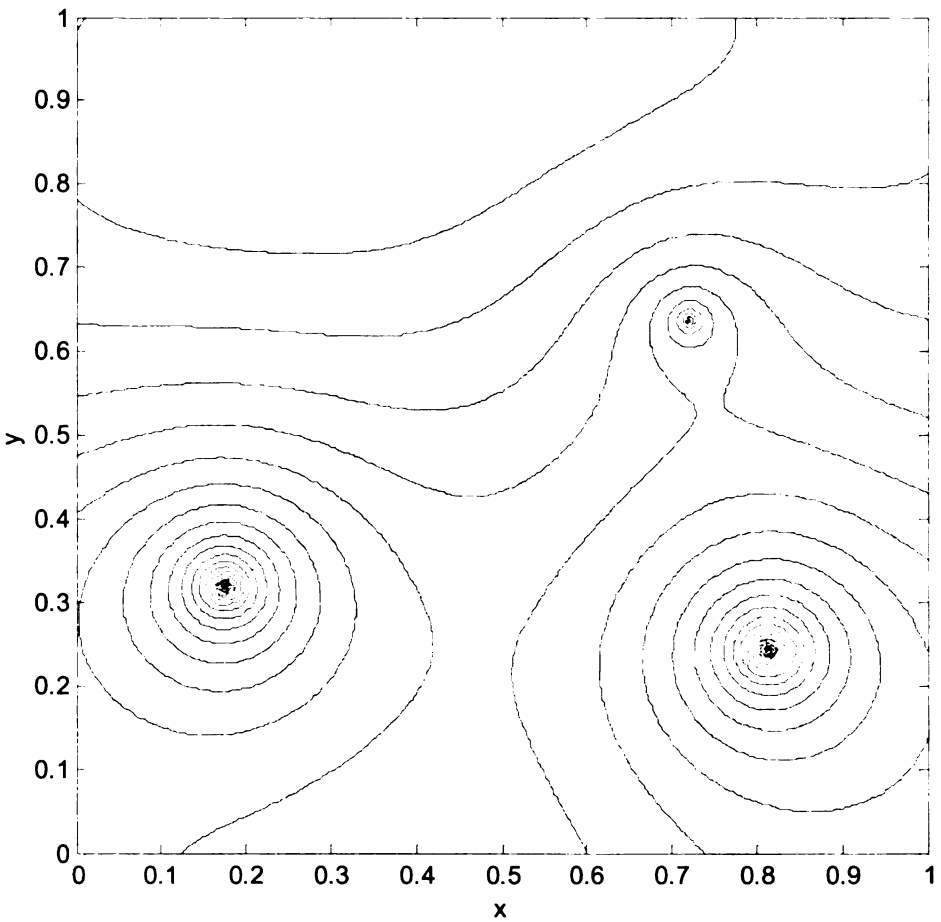

Figure 2.7: Oxygen concentration level curve at $t = 10$, transient state, three capillaries with random characteristics

Chapter 3

Substrate Transport in Multi-capillary Beds with Axial Diffusion

Radial diffusion may have considerably more effect than axial diffusion for oxygen transport for long and parallel capillary bed. In Krogh's initial work the tissue area was taken as a coaxial cylinder around a single capillary, and axial diffusion was neglected in the elementary mathematical solution. Salathe and Wang [24] studied and presented solutions including axial diffusion for a single capillary and its coaxial Krogh cylinder. Previous work from them suggests oxygen concentrations surrounding single capillaries as well as linear oxyhemoglobin dissociation relationship clearly indicates the axial diffusion may have significant effect on oxygen transport profiles. It is therefore tempting and beneficial to have a full analysis of substrate diffusion under effect of axial diffusion.

In this chapter we will make attempts to extend the solutions with axial diffusion to multicapillary beds inside a tissue cylinder, where arbitrary characteristics including random locations and uneven oxygen strength are taken into account. Methods are used following the scheme presented by Salate and Wang in their paper. Review

of the model and further analysis for multicapillary region will be given first. Further discussion of the solutions for oxygen supply on multicapillary beds near the arterial end, in the central region of capillary and near the venous end will be introduced in the remainder of the chapter. The prime model we use here is similar to what has been introduced in the previous chapter except that a Z axis is added and circular cylindrical tissue around multiple capillaries is employed. In order for us to apply relatively small longitudinal diffusivities, perturbation method is utilized to solve the associated governing equations.

3.1 Problem Review and Analysis

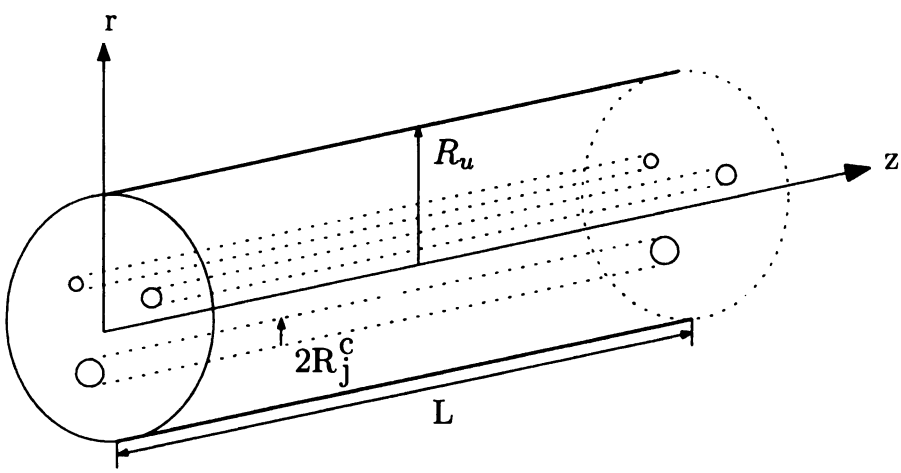

Figure 3.1: Uneven locations and diffusion strength N capilary bed surrounded by a cylinder of tissue

3.1.1 Formulation

Consider n number of capillaries surrounded by a cylinder of tissue having radius R_u. The capillaries are parallel to each other and have length L and radius R_j^c, where $1 \leq j \leq n$. The oxygen is diffused from the capillaries to the tissue which consumes oxygen at a constant rate κ per volume of tissue. Let z and r denote the centered axes

along the capillary direction and radial direction both normalized with respect to L, $0 \leq z \leq 1$, and R_u,$0 \leq r \leq 1$. The governing equation for the oxygen concentration in the tissue $c_u(r, \theta, z)$ follows

$$\frac{1}{r}\frac{\partial}{\partial r} r \frac{\partial c}{\partial r} + \frac{1}{r^2}\frac{\partial^2 c}{\partial \theta^2} + \varepsilon^2 \frac{\partial^2 c}{\partial z^2} = \kappa_0, \quad r \leq 1, \quad 0 \leq z \leq 1, \tag{3.1}$$

where $c = c_u/C_A$ is nondimensionalized with respect to the oxygen concentration of the arterial blood, C_A. And $\varepsilon = \sqrt{D_z/D_r}(R_u/L)$, $R_j = R_j^c/R_u$, $\kappa_0 = R_u^2\kappa/D_r C_A$. Here D_r, D_z are the radial and axial diffusivities of the tissue.

On the boundary of the region we require no flux

$$\frac{\partial c}{\partial r} = 0, \quad r = 1, \quad 0 \leq z \leq 1 \tag{3.2}$$

$$\frac{\partial c}{\partial z} = 0, \quad z = 0, 1, \quad r \leq 1 \tag{3.3}$$

Within the jth capillary, the oxygen substrate per unit volume of blood C_j^o depends on the quantity of dissolved oxygen C_j and oxygen capacity in blood cells. Denote the oxygen capacity at 100% saturation by V_C and the oxyhemoglobin dissociation curve gives a relationship that can be approximated by

$$S(C_j)^* = \frac{K(C_A C_j)^\lambda}{1 + K(C_A C_j)^\lambda} \tag{3.4}$$

The relationship here states that as the dissolved oxygen increases the rate tends to approach 1 for large quantity and grow dramatically for small amount of oxygen. Alternative forms can be found in Meldon [29]. Particular forms of the representation of oxyhemoglobin dissociation does not affect the analysis. A linear form of C_j^o is

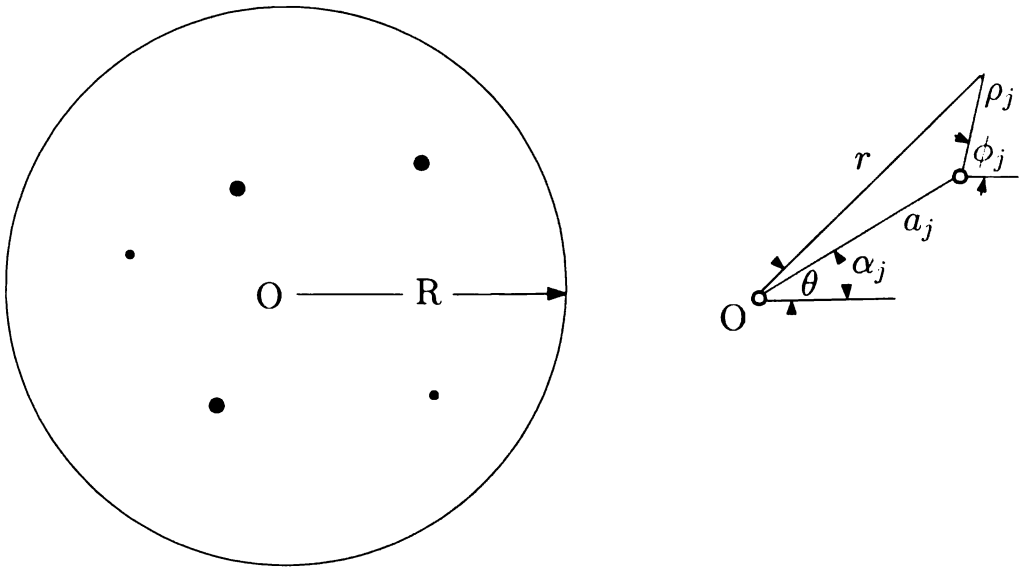

(a) (b)

Figure 3.2: (a) General distribution of capillaries in the circular perpendicular cut, (b)The coordinate system. O reprensents the origin of the polar coordinates

then given by $C_j + V_c S(C_j)^*$ (Salathe and Wang [24]).

The governing equation for the rate of oxygen concentration within the jth capillary at location z $(0 \leq z \leq 1)$ is

$$\frac{d}{dz}[C_j + VS(C_j)] = \gamma \oint \frac{\partial c}{\partial \rho_j}\Big|_{\rho_j = R_j} d\phi + \varepsilon^2 \nu \frac{d^2 C_j}{dz^2} \tag{3.5}$$

where $\gamma = 2\pi D_T L R_j / Q$ and $\nu = R_j D_p / 2 D_z \gamma$. Q is the blood flow rate and D_p is the diffusivity in blood. The first term on the right states the oxygen rate of blood diffusing from the jth capillary to surrounding tissue as axial diffusion and the second term on the right represents the longitudinal diffusion along the z axis. The oxygen concentration at the arterial end is

$$C_j(0) = 1 \tag{3.6}$$

3.1.2 Perturbation of Substrate Concentration

Eq (3.5) will be solved for $R_j \ll 1$ and $\varepsilon \ll 1$. The equation shows that the axial diffusion tends to become negligible as if $\varepsilon \to 0$. For $\varepsilon = 0$, it reduces to a 2-dimensional problem neglecting axial diffusion which gives the dominant effect on oxygen concentration in tissue and capillaries. Perturbation technique will be used for higher order of ε ($\varepsilon \ll 1$) and corresponding solutions will give the effect of axial diffusion.Let $C(z) = C_j(z)$. The solution for $C(z)$ and $c(r, \theta, z)$ will be obtained in the form of an asymptotic series, for small ε.

$$\begin{aligned} C(z) &\sim C_0(z) + \varepsilon^2 C_1(z) + ... \\ c(r,\theta,z) &\sim c_0(r,\theta,z) + \varepsilon^2 c_1(r,\theta,z) + ... \end{aligned} \tag{3.7}$$

The oxyhemoglobin dissociation relationship can be expanded for small ε by using Taylor series expansion to obtain

$$S(C_0 + \varepsilon^2 C_1) = S(C_0) + \varepsilon^2 C_1 S'(C_0) + ... \tag{3.8}$$

By letting $\varepsilon = 0$, the equations for the leading terms $C_0(z)$ and $c_0(r, \theta, z)$ along with the boundary conditions at the arterial end, capillary wall and outer boundary of cylindrical cut are

$$\frac{1}{r}\frac{\partial}{\partial r} r \frac{\partial c_0}{\partial r} + \frac{1}{r^2}\frac{\partial^2 c_0}{\partial \theta^2} = \kappa, \quad r \le 1, \quad z \le 1, \tag{3.9}$$

$$\frac{\partial c_0}{\partial r}|_{r=1} = 0, \qquad z \le 1 \tag{3.10}$$

$$\frac{\partial c_0}{\partial z}|_{z=0} = 0, \quad \frac{\partial c_0}{\partial z}|_{z=1} = 0 \quad r \le 1 \tag{3.11}$$

$$\frac{d}{dz}[C_0 + VS(C_0)] = \gamma \int_0^{2\pi} \frac{\partial c_0}{\partial \rho}\Big|_{\rho=R_u} d\phi \tag{3.12}$$

$$C_0(0) = 1 \tag{3.13}$$

We then need to give solutions to for $C_0(z)$ and $c_0(r,\theta,z)$ to the above equations. For c_0, the oxygen concentration in tissue, here we employ matching technique similar to the results from the previous chapter. It follows from Eqs (3.9) to (3.11) that

$$\begin{aligned} c_0(r,\theta,z) = r^2/4 + \sum_{j=1}^{N} \{C_{0,j} - \kappa/4 \cdot \ln[r^2 + a_j^2 - 2ra_j\cos(\theta - \alpha_j)]\} \\ + \kappa \cdot \sum_{n=0}^{\infty} r^n (A_n \cos n\theta + B_n \sin n\theta) \end{aligned} \tag{3.14}$$

where A_n and B_n are constant coefficients that (see Appendix A)

$$A_n = \frac{1}{2n} \sum_{j=1}^{N} a_j^n \cos(n\alpha_j), \quad n \geq 1 \tag{3.15}$$

$$B_n = \frac{1}{2n} \sum_{j=1}^{N} a_j^n \sin(n\alpha_j), \quad n \geq 1 \tag{3.16}$$

The solution states that the oxygen concentration in tissue is a combination of oxygen diffusion from each capillary within the circular region $0 \leq r \leq 1$. ρ_j is the distance from the j th capillary. The effect of oxygen diffusion from j th capillary diminishes as ρ_j increases. A_0 is a constant due to Nuemann boundary condition and can be set to make $c_0 > 0$. This analytical solution gives sufficiently good description of oxygen concentration in the cylindrical cross section. Substitute (3.14) into Eq. (3.12). It follows from boundary condition (3.13) that the solution for C_0, the leading term of $C(z)$ by letting $\varepsilon = 0$

$$C_0 + VS(C_0) = \left[\pi\gamma\left(R - \frac{\kappa}{R} - N\right) + \widehat{\varphi_0}(R)\right] \cdot z + VS(1) + 1 \tag{3.17}$$

where N is the number of capillaries. and $\widehat{\varphi_0}(R)$ follows (see Appendix B)

$$\widehat{\varphi_0}(R) = \sum_{j=1}^{N} a_j^2 \kappa \cdot \pi R + o(R) \quad for \quad R \ll 1 \tag{3.18}$$

The oxygen concentration in capillary $C_0(z)$ can be obtained from Eq. (3.17) due to monotonity of the oxyhemoglobin dissociation function $S(C)$.

The equations for the second term $c_1(r, \theta, z)$ and $C_0(z)$ can be obtained by substituting Eq. (3.7) into Eqs. (3.1), (3.2), (3.3), (3.5) and (3.6) and retaining terms of order ε^2. (3.8) gives

$$\frac{1}{r}\frac{\partial}{\partial r} r \frac{\partial c_1}{\partial r} + \frac{1}{r^2}\frac{\partial^2 c_1}{\partial \theta^2} = -\frac{\partial^2 c_0}{\partial z^2}, \quad r \le 1, \quad z \le 1, \tag{3.19}$$

$$\frac{\partial c_1}{\partial r}|_{r=1} = 0, \qquad z \le 1 \tag{3.20}$$

$$\frac{\partial c_1}{\partial z}|_{z=0} = 0, \quad \frac{\partial c_1}{\partial z}|_{z=1} = 0 \quad r \le 1 \tag{3.21}$$

$$\frac{d}{dz} C_1[1 + VS'(C_0)] = \gamma \int_0^{2\pi} \frac{\partial c_1}{\partial \rho}\Big|_{\rho=R} d\phi + \nu \frac{d^2 C_0}{dz^2}, \quad 0 < z < 1 \tag{3.22}$$

$$C_1(0) = 0 \tag{3.23}$$

which includes the effect of axial diffusion. The solution for $c_1(r, \theta, z)$ to Eq. (3.19) satisfying boundary conditions (3.20) and (3.21)is found to be

$$\begin{aligned} c_1(r, \theta, z) = r^2/4 + & \sum_{j=1}^{N} \{C_{1,j} + C_0''(z)/4 \cdot \ln[r^2 + a_j^2 - 2ra_j \cos(\theta - \alpha_j)]\} \\ & - C_0''(z) \cdot \sum_{n=0}^{\infty} r^n (A_n \cos n\theta + B_n \sin n\theta) \end{aligned} \tag{3.24}$$

where A_n and B_n are constant coefficients that

$$A_n = \frac{1}{2n} \sum_{j=1}^{N} a_j^n \cos(n\alpha_j), \quad n \geq 1 \tag{3.25}$$

$$B_n = \frac{1}{2n} \sum_{j=1}^{N} a_j^n \sin(n\alpha_j), \quad n \geq 1 \tag{3.26}$$

In the above solution, the zeroth order term $C_0(z)$ has already been found in (3.17). At this point, the oxygen concentration $c = c_0 + \varepsilon^2 c_1$ at any location z in the tissue cylinder around N number of capillaries is completely known. For the oxygen concentration in capillary $C = C_0 + \varepsilon^2 C_1$ including axial diffusion, similar to what we achieved above, substitute (3.24) into Eq.(3.22) with boundary condition (3.23). It follows

$$\begin{aligned} C_1[1 + VS'(C_0(z))] = & \left[\pi\gamma\,(R - N)\right] \cdot z \\ & + \left(\nu - \widehat{\varphi_1}(R) + \frac{\pi\gamma}{R}\right) \cdot [C_0'(z) - C_0'(0)] \\ & + C_1(0)[1 + VS'(1)] \end{aligned} \tag{3.27}$$

where N is the number of capillaries. and $\widehat{\varphi_1}(R)$ follows

$$\widehat{\varphi_1}(R) = \sum_{j=1}^{N} a_j^2 \cdot \pi R + o(R) \quad for \quad R \ll 1 \tag{3.28}$$

C_1 can be obtained from above because $S(C)$ is monotone and concave down. The solutions are valid throughout the cylindrical region except when it is near $z = 0$. At the arterial end of the cylinder radial, diffusion D_T and axial diffusion D_p are of equal importance. Therefore the small perturbation ε^2 can not be employed for z near zero, and the solutions from (3.27) and boundary condition (3.23) are no longer valid. The expansions needs to be adjusted for a small layer near $z = 0$ and to satisfy the boundary condition with no flux through the end of the cylinder.

3.1.3 Small z Boundary Layer

For small z, there exists a boundary layer where solutions shall be constructed differently. The length of the layer diminishes in the sense of $\varepsilon \to 0$. Instead of z, use $Z = z/\varepsilon$ ($z \to 0$ as $\varepsilon \to 0$ for fixed Z) as the variable for this boundary layer. The new functions of oxygen concentration in tissue and capillary become now $\widetilde{c}(r,\theta,Z) = c(r,\theta,\varepsilon Z)$ and $\widetilde{C}(Z) = C(\varepsilon Z)$ The governing equations are

$$\frac{1}{r}\frac{\partial}{\partial r} r \frac{\partial \widetilde{c}}{\partial r} + \frac{1}{r^2}\frac{\partial^2 \widetilde{c}}{\partial \theta^2} + \frac{\partial^2 \widetilde{c}}{\partial Z^2} = \kappa, \quad r \le 1, \quad Z \ge 0, \tag{3.29}$$

$$\frac{d}{dz}[\widetilde{C} + VS(\widetilde{C})] = \varepsilon\,\gamma \int_0^{2\pi} \frac{\partial \widetilde{c}}{\partial \rho}\Big|_{\rho=R} d\phi + \varepsilon\,\nu \frac{d^2\widetilde{C}}{dZ^2}, \quad Z \ge 0 \tag{3.30}$$

$$\frac{\partial \widetilde{c}}{\partial r}|_{r=1} = 0, \qquad z \le 1 \tag{3.31}$$

$$\frac{\partial \widetilde{c}}{\partial Z}|_{Z=0} = 0, \qquad r \le 1 \tag{3.32}$$

$$\widetilde{C}(0) = 1 \tag{3.33}$$

Eq. (3.30) can be written as

$$\frac{d}{dz}[\widetilde{C} + VS(\widetilde{C})] = \varepsilon\,\gamma \int_0^{2\pi} \frac{\partial \widetilde{c}_p + \widetilde{c}_s + \widetilde{c}_h}{\partial \rho}\Big|_{\rho=R} d\phi + \varepsilon\,\nu \frac{d^2\widetilde{C}}{dZ^2}, \quad Z \ge 0 \tag{3.34}$$

where $\widetilde{c}_p$, $\widetilde{c}_p$, $\widetilde{c}_p$ give respectively the particular solution, source solution and homogenous solution of oxygen concentration in tissue. Further discussion of the explicit expressions will be given in the next section.

The solutions of $\widetilde{c}(r,\theta,Z)$ and $\widetilde{C}(Z)$ near $z = 0$ should be uniformly consistent to what has been achieved from solutions throughout cylinder outside the boundary layer. To satisfy

$$\lim_{Z\to\infty} \widetilde{c}(r,\,\theta,\,Z) \;=\; \lim_{z\to 0} c\,(r,\,\theta,\,z) \tag{3.35}$$

$$\lim_{Z\to\infty} \widetilde{C}\,(Z) \;=\; \lim_{z\to 0} C\,(z) \tag{3.36}$$

it is necessary to look at the solutions of $c(r,\theta,Z)$ and $C(Z)$ near the boundary layer at $z=0$ and match the inside solutions $\widetilde{C}$, $\widetilde{c}$ to the outside solution C , c at the first few orders of ε. Write $c(r,\theta,Z) + \varepsilon^2 c(r,\theta,Z)$ and $C(Z) + \varepsilon^2 C(Z)$ in terms of r,θ and Z and expand in terms of ε

$$C(\varepsilon Z) \;=\; C(0) + \varepsilon\mu_1 Z + \varepsilon^2\mu_2 Z + o(\varepsilon^3) \tag{3.37}$$

where $\mu_1 = C_0'(0)$ and $mu_2 = C_0''(0)/2$. Expand $C_0(\varepsilon Z) + VS(C_0(\varepsilon Z))$ using Taylor expansion

$$\begin{aligned} C_0(\varepsilon Z) + VS(C_0(\varepsilon Z)) \;=& 1 + VS(1) \\ &+ \varepsilon\,\mu_1(1 + VS'(1))Z \\ &+ \varepsilon^2\left[(1 + VS'(1))\mu_2 + \frac{VS''(1)}{2}\mu_1^2\right] Z^2 \\ &+ O(\varepsilon^3) \end{aligned} \tag{3.38}$$

From (3.17), $C_0(\varepsilon Z) + VS(C_0(\varepsilon Z))$ can be explicitly written as

$$\begin{aligned} C_0(\varepsilon Z) + VS(C_0(\varepsilon Z)) \;=& 1 + VS(1) \\ &+ \varepsilon\left[\pi\,\gamma\,(R - \frac{\kappa}{R} - N) + \widehat{\varphi_0}(R)\right] Z \end{aligned} \tag{3.39}$$

Compare (3.38) with (3.39). μ_1 and μ_2 are found to be respectively

$$\mu_1 \;=\; \frac{\pi\,\gamma\,(R - \frac{\kappa}{R} - N) + \widehat{\varphi_0}(R)}{1 + VS'(1)} \tag{3.40}$$

$$\mu_2 = -\frac{VS''(1)\left[\pi\gamma\left(R-\frac{\kappa}{R}-N\right)+\widehat{\varphi_0}(R)\right]^2}{2\Big(1+VS'(1)\Big)^3} \tag{3.41}$$

where $\widehat{\varphi_0}(R)$ is given in (3.18). The oxygen concentration in capillaries are approximated to the order of ε^2. Add the C_1 term to the above

$$\begin{aligned} C(z) &\sim C_0(z)+\varepsilon^2 C_1(z) \\ &\sim 1+\varepsilon\,\mu_1 Z+\varepsilon^2\left(\mu_2 Z^2+C_1(0)\right)+O(\varepsilon^3) \end{aligned} \tag{3.42}$$

where μ_1 and μ_2 are given in (3.40) and (3.41). The oxygen concentration in tissue $c_0(r,\theta,z)+\varepsilon^2 c_1(r,\theta,z)$ can be expanded as

$$\begin{aligned} c\,(r,\theta,z) &\sim c_0(r,\theta,z)+\varepsilon^2 c_1(r,\theta,z) \\ &\sim N+r^2/4-\kappa/4\cdot\sum_{j=1}^{N}\ln[r^2+a_j^2-2ra_j\cos(\theta-\alpha_j)] \\ &\quad+\kappa\sum_{n=0}^{\infty}r^n(A_n\cos n\theta+B_n\sin n\theta)+\varepsilon\sum_{j=1}^{N}\mu_{1,j}\,Z \\ &\quad+\varepsilon^2\Bigg\{\mu_2 Z^2+r^2/4+\sum_{j=1}^{N}C_{1,j}(0) \\ &\quad+\mu_2/2\cdot\sum_{j=1}^{N}\ln[r^2+a_j^2-2ra_j\cos(\theta-\alpha_j)] \\ &\quad-2\mu_2\sum_{n=0}^{\infty}r^n(A_n\cos n\theta+B_n\sin n\theta)\Bigg\}+O(\varepsilon^3) \end{aligned} \tag{3.43}$$

where (to j th capillary)

$$\mu_{1,j} = \frac{\pi\gamma\left(R_j-\frac{\kappa}{R_j}-N\right)+\widehat{\varphi_0}(R_j)}{1+VS'(1)} \tag{3.44}$$

To match the boundary layer solutions to outside solutions C and c, expansions

of $\widetilde{C}$ and $\widetilde{c}$ in terms of ε must be in the form

$$\widetilde{C}(z) \sim 1 + \varepsilon \mu_1 Z + \varepsilon^2 H(Z) \tag{3.45}$$

$$\begin{aligned}\widetilde{c}(z) \sim\ & N + r^2/4 - \kappa/4 \cdot \sum_{j=1}^{N} \ln[r^2 + a_j^2 - 2ra_j \cos(\theta - \alpha_j)] \\ & + \kappa \sum_{n=0}^{\infty} r^n (A_n \cos n\theta + B_n \sin n\theta) \\ & + \varepsilon \psi(r, \theta, Z) \\ & + \varepsilon^2 \varphi(r, \theta, Z)\end{aligned} \tag{3.46}$$

$H(Z)$, $\psi(r, \theta, Z)$ and $\varphi(r, \theta, Z)$ are to be determined. Use the expansions given above (3.45) and (3.46) substitute into the Eqs. (3.29) and (3.30) with boundary conditions (3.31) to (3.34). Match first and second order ε terms corresponding to $\widetilde{C}$ and $\widetilde{c}$. The set of differential equations for $H(Z)$, $\psi(r, \theta, Z)$ and $\varphi(r, \theta, Z)$ are

I. For $H(z)$, after matching the ε^2 terms from Eq. (3.30)

$$\frac{dH}{dZ} = 2\mu_2 Z + \frac{\gamma}{1 + VS'(1)} \oint \frac{\partial \psi}{\partial \rho}\Big|_{\rho \to R} d\phi \tag{3.47}$$

$$H(0) = 0 \tag{3.48}$$

and in order to match the outside solution $C(z)$ (3.42) for $O(\varepsilon)$ terms

$$\lim_{Z \to \infty} H(Z) = \mu_2 Z^2 + C_1(0) \tag{3.49}$$

II. For $\psi(r, \theta, Z)$, after matching corresponding terms with respect to ε

$$\frac{1}{r} \frac{\partial}{\partial r} r \frac{\partial \psi}{\partial r} + \frac{1}{r^2} \frac{\partial^2 \psi}{\partial \theta^2} + \frac{\partial^2 \psi}{\partial Z^2} = 0, \quad r \le 1, \quad Z \ge 0, \tag{3.50}$$

$$\frac{\partial \psi}{\partial r}\Big|_{r=1} = 0, \qquad Z \ge 0 \tag{3.51}$$

$$\frac{\partial \psi}{\partial Z}|_{Z=0} = 0, \qquad r \leq 1 \tag{3.52}$$

$$\widehat{C}_{\psi}(r, \theta, Z) = \mu_1 Z, \quad at \ \rho = R, \quad Z \geq 0 \tag{3.53}$$

where $\widehat{C}_{\psi}$ is the capillary source concentration associated with ψ and in order to match the outside solution $c(r, \theta, z)$ (3.43) at ε term, where $\mu_{1,j}$ is defined in (3.44)

$$\lim_{Z \to \infty} \psi = \sum_{j=1}^{N} \mu_{1,j} Z \tag{3.54}$$

III. For $\varphi(r, \theta, Z)$, after matching corresponding terms with respect to ε

$$\frac{1}{r} \frac{\partial}{\partial r} r \frac{\partial \varphi}{\partial r} + \frac{1}{r^2} \frac{\partial^2 \varphi}{\partial \theta^2} + \frac{\partial^2 \varphi}{\partial Z^2} = 0, \quad r \leq 1, \quad Z \geq 0, \tag{3.55}$$

$$\frac{\partial \varphi}{\partial r}|_{r=1} = 0, \qquad Z \geq 0 \tag{3.56}$$

$$\frac{\partial \varphi}{\partial Z}|_{Z=0} = 0, \qquad r \leq 1 \tag{3.57}$$

$$\widehat{C}_{\varphi}(r, \theta, Z) = H(Z), \quad at \ \rho = R, \quad Z \geq 0 \tag{3.58}$$

where $\widehat{C}_{\varphi}$ is the capillary source concentration associated with ψ and in order to match the outside solution $C(z)$ (3.43) for $O(\varepsilon^2)$ terms

$$\begin{aligned} \lim_{Z \to \infty} \varphi = \ & \mu_2 Z^2 + r^2/4 + \sum_{j=1}^{N} C_{1,j}(0) \\ & + \mu_2/2 \cdot \sum_{j=1}^{N} \ln[r^2 + a_j^2 - 2 r a_j \cos(\theta - \alpha_j)] \\ & - 2\mu_2 \sum_{n=0}^{\infty} r^n (A_n \cos n\theta + B_n \sin n\theta) \end{aligned} \tag{3.59}$$

From Eq.(3.47) and boundary condition (3.48)

$$H(Z) = \mu_2^2 Z + \frac{\gamma}{1+VS'(1)} \int_0^Z \oint \frac{\partial \psi}{\partial \rho}\Big|_{\rho \to R} d\phi \, dZ \tag{3.60}$$

Substitute (3.60) into matching condition (3.49), then

$$C_1(0) = \frac{\gamma}{1+VS'(1)} \int_0^\infty \oint \frac{\partial \psi}{\partial \rho}\Big|_{\rho \to R} d\phi \, dZ \tag{3.61}$$

3.2 Further Discussion on Matching Solutions

In order to successfully match the inner solution with the outer solution inside the cylindrical tissue region, we need to obtain the solutions for perturbation functions ψ and φ. To obtain the solutions for ψ, let

$$\psi = \sum_{j=1}^{N} \widehat{C}_j(z) - 1/2\Big(\ln \rho_j - \ln R_j\Big) + T(r, \theta, Z) \tag{3.62}$$

where $\widehat{C}_j(z) = \mu_{1,j} Z$. The first two terms in (3.62) gives the combination of oxygen diffusion from each capillary source. The function, T, defined in the semi infinite cylinder $r \leq 1$, $Z \geq 0$ satisfies the Laplace's Equation

$$\frac{\partial^2 T}{\partial r^2} + \frac{1}{r}\frac{\partial T}{\partial r} + \frac{1}{r^2}\frac{\partial^2 T}{\partial \theta^2} + \frac{\partial^2 T}{\partial Z^2} = 0, \quad r \leq 1, \quad Z \geq 0, \tag{3.63}$$

$$\frac{\partial T}{\partial r} = \frac{\partial}{\partial r}(1/2 \sum_{j=1}^{N} \ln \rho_j), \qquad at \quad r = 1 \tag{3.64}$$

$$\frac{\partial T}{\partial Z}|_{Z=0} = -\sum_{j=1}^{N} \mu_{1,j}, \qquad r \leq 1 \tag{3.65}$$

Notice that on the outer boundary $r = 1$, T has no flux in or out of the cylindrical region. T satisfies a well posed problem that can be solved first by separation of

variables.

$$T(r,\theta,Z) = R(r)\,\Theta(\theta)\,\Gamma(Z) \tag{3.66}$$

then for some unknown constant λ, we have

$$\frac{1}{\Gamma}\,\Gamma'' = \lambda^2, \qquad \frac{1}{\Theta}\frac{\partial^2\Theta}{\partial\theta^2} = -n^2 \tag{3.67}$$

$$r^2\frac{\partial^2 R}{\partial r^2} + r\frac{\partial R}{\partial r} + (r^2\lambda - n^2)R = 0 \tag{3.68}$$

The Eq (3.63) is reduced to a Helmholtz equation in two variables, with circular supports. T is then solved to be in a general form

$$T(r,\theta,Z) = \int_0^\infty e^{-\lambda Z}\sum_{n=0}^{\infty}\Big\{\Big[A_n(\lambda)\sin(n\theta) + B_n(\lambda)\cos(n\theta)\Big] \cdot\Big[D_n J_n(\lambda r) + E_n Y_n(\lambda r)\Big]\Big\}\,d\lambda \tag{3.69}$$

where J_* and Y_* are Bessel functions of the first and second kind. and $A_n(\lambda)$,$B_n(\lambda)$,$D_n(\lambda)$ and $E_n(\lambda)$ are constants which are limited to the boundary conditions.

The radial derivative of Eq. (3.69) is

$$\frac{\partial T}{\partial r} = \int_0^\infty e^{-\lambda Z}\sum_{n=0}^{\infty}\Big\{\Big[\widehat{A}_n(\lambda)\sin(n\theta) + \widehat{B}_n(\lambda)\cos(n\theta)\Big] \cdot\lambda\Big[\widehat{D}_n(\lambda)\Big(J_{n-1}(\lambda r) - J_{n+1}(\lambda r)\Big) + \widehat{E}_n(\lambda)\Big(Y_{n-1}(\lambda r) - Y_{n+1}(\lambda r)\Big)\Big]\Big\}\,d\lambda \tag{3.70}$$

The boundary condition (3.64) gives at $r = 1$

$$\frac{\partial T}{\partial r} = \sum_{j=1}^{N} \frac{r - a_j \cos(\theta - \alpha_j)}{r^2 + a_j^2 - 2ra_j \cos(\theta - \alpha_j)} \tag{3.71}$$

$\Rightarrow$

$$\begin{aligned} &\sum_{j=1}^{N} \frac{1 - a_j \cos(\theta - \alpha_j)}{1 + a_j^2 - 2a_j \cos(\theta - \alpha_j)} \\ &= \int_0^{\infty} e^{-\lambda Z} \sum_{n=0}^{\infty} \left\{ \left[\widehat{A}_n(\lambda) \sin(n\theta) + \widehat{B}_n(\lambda) \cos(n\theta) \right] \right. \\ &\quad \left. \cdot \lambda \begin{bmatrix} \widehat{D}_n(\lambda) \Big(J_{n-1}(\lambda) - J_{n+1}(\lambda) \Big) \\ + \widehat{E}_n(\lambda) \Big(Y_{n-1}(\lambda) - Y_{n+1}(\lambda) \Big) \end{bmatrix} \right\} d\lambda \end{aligned} \tag{3.72}$$

Multiply the above equation by $\cos(m\theta)$ and integrate from 0 to 2π with respect to θ yield

$$\frac{\partial T}{\partial r} = \sum_{j=1}^{N} \frac{r - a_j \cos(\theta - \alpha_j)}{r^2 + a_j^2 - 2ra_j \cos(\theta - \alpha_j)} \tag{3.73}$$

$\Rightarrow$

$$\begin{aligned} &\widehat{B}_m \pi \int_0^{\infty} e^{-\lambda Z} \cdot \lambda \begin{bmatrix} \widehat{D}_m(\lambda) \Big(J_{m-1}(\lambda) - J_{m+1}(\lambda) \Big) \\ + \widehat{E}_n(\lambda) \Big(Y_{m-1}(\lambda) - Y_{m+1}(\lambda) \Big) \end{bmatrix} d\lambda \\ &= \sum_{j=1}^{N} \int_0^{2\pi} \frac{1 - a_j \cos(\theta - \alpha_j)}{1 + a_j^2 - 2a_j \cos(\theta - \alpha_j)} \cos(m\theta) d\theta \end{aligned} \tag{3.74}$$

Letting $\vartheta = \theta - \alpha_j$ and using integration formulas in Gradshteyn and Ryzhik [27], it yields

$$\widehat{B}_m \pi \int_0^{\infty} e^{-\lambda Z} \cdot \lambda \begin{bmatrix} \widehat{D}_m(\lambda)\Big(J_{m-1}(\lambda) - J_{m+1}(\lambda)\Big) \\ +\widehat{E}_n(\lambda)\Big(Y_{m-1}(\lambda) - Y_{m+1}(\lambda)\Big) \end{bmatrix} d\lambda$$

$$= \sum_{j=1}^{N} \int_0^{2\pi} \frac{1 - a_j \cos(\theta - \alpha_j)}{1 + a_j^2 - 2a_j \cos(\theta - \alpha_j)} \cos m\theta \, d\theta$$

$$= \sum_{j=1}^{N} \int_0^{2\pi} \frac{1 - a_j \cos(\theta - \alpha_j)}{1 + a_j^2 - 2a_j \cos(\theta - \alpha_j)} \begin{bmatrix} \cos(m\vartheta)\cos(m\alpha_j) \\ -\sin(m\vartheta)\sin(m\alpha_j) \end{bmatrix} d\vartheta$$

$$= \sum_{j=1}^{N} \pi a_j^m \cos(m\alpha_j), \qquad m \geq 1 \tag{3.75}$$

and thus, we can achieve

$$\widehat{B}_m = \frac{\sum_{j=1}^{N} a_j^m \cos(m\alpha_j)}{G_m(Z)} \tag{3.76}$$

where

$$G_m(Z) = \int_0^{\infty} e^{-\lambda Z} \cdot \lambda \begin{bmatrix} \widehat{D}_m(\lambda)\Big(J_{m-1}(\lambda) - J_{m+1}(\lambda)\Big) \\ +\widehat{E}_n(\lambda)\Big(Y_{m-1}(\lambda) - Y_{m+1}(\lambda)\Big) \end{bmatrix} d\lambda \tag{3.77}$$

In the same manner, multiply Eq. (3.74) by $\sin(m\theta)$ and integrate from 0 to 2π with respect to θ. It yields

$$\begin{aligned}
&\hat{A}_m \pi \int_0^{\infty} e^{-\lambda Z} \cdot \lambda \begin{bmatrix} \hat{D}_m(\lambda)\Big(J_{m-1}(\lambda) - J_{m+1}(\lambda)\Big) \\ +\hat{E}_n(\lambda)\Big(Y_{m-1}(\lambda) - Y_{m+1}(\lambda)\Big) \end{bmatrix} d\lambda \\
&= \sum_{j=1}^{N} \int_0^{2\pi} \frac{1 - a_j \cos(\theta - \alpha_j)}{1 + a_j^2 - 2a_j \cos(\theta - \alpha_j)} \sin(m\theta) d\theta \\
&= \sum_{j=1}^{N} \int_0^{2\pi} \frac{1 - a_j \cos(\theta - \alpha_j)}{1 + a_j^2 - 2a_j \cos(\theta - \alpha_j)} \begin{bmatrix} \sin(m\vartheta)\cos(m\alpha_j) \\ +\cos(m\vartheta)\sin(m\alpha_j) \end{bmatrix} d\vartheta \\
&= \sum_{j=1}^{N} \pi a_j^m \sin(m\alpha_j), \qquad m \geq 1
\end{aligned} \tag{3.78}$$

and thus, we can achieve

$$\hat{A}_m = \frac{\sum_{j=1}^{N} a_j^m \sin(m\alpha_j)}{G_m(Z)} \tag{3.79}$$

The axial derivative of Eq. (3.69) is

$$\begin{aligned}
&\frac{\partial T}{\partial Z}|_{Z=0} = \sum_{j=1}^{N} \mu_{1,j} \\
&= \int_0^{\infty} (-\lambda) \sum_{n=0}^{\infty} \frac{\hat{D}_n(\lambda) J_n(\lambda r) + \hat{E}_n(\lambda) Y_n(\lambda r)}{G_n(Z)} \sum_{j=1}^{N} a_j^n \begin{bmatrix} (\sin(n\alpha_j)\sin(n\theta) \\ +\cos(n\alpha_j)cos(n\theta)\Big) \end{bmatrix} d\lambda
\end{aligned} \tag{3.80}$$

$\hat{D}_n$ and $\hat{E}_n$ can be solved in terms of an eigenfunction expansion involving Bessel

functions, where the set of eigenfunctions is

$$\Big\{J_n(\lambda r)\sin(n\theta),\quad Y_n(\lambda r)\sin(n\theta),\quad J_n(\lambda r)\cos(n\theta),\quad Y_n(\lambda r)\cos(n\theta)\Big\}$$

Then ψ, which describes the oxygen concentration near the arterial boundary layer to the first order of ε can be expressed as

$$\begin{aligned}\psi &= \sum_{j=1}^{N} \widehat{C}_j(z) - 1/2\Big(\ln\rho_j - \ln R_j\Big) \\ &\quad + \int_0^{\infty} \sum_i \sum_{n=0}^{\infty} A_{i,n}(\lambda) f_{i,n}(r,\theta) e^{-\lambda Z} d\lambda \end{aligned} \tag{3.81}$$

where

$$A_{i,n} \in \left\{ \begin{array}{l} \widehat{A}_n\widehat{D}_n \\ \widehat{A}_n\widehat{E}_n \\ \widehat{B}_n\widehat{D}_n \\ \widehat{B}_n\widehat{E}_n \end{array} \right\} \quad \textit{and} \quad f_{i,n}(r,\theta) \in \left\{ \begin{array}{l} J_n(\lambda r)\sin(n\theta) \\ Y_n(\lambda r)\sin(n\theta) \\ J_n(\lambda r)\cos(n\theta) \\ Y_n(\lambda r)\cos(n\theta) \end{array} \right\}$$

The function $H(Z)$ for the oxygen concentration in capillaries can then be determined by substituting the solution for $\psi(r,\theta,Z)$ into Eq. (3.60)

$$H(Z) = \mu_2^2 Z + C_1(0) + \frac{\gamma}{1+VS'(1)} \int_0^Z \oint \frac{\partial\psi}{\partial\rho}\Big|_{\rho\to R} d\phi\, dZ \tag{3.82}$$

The third term in ψ is well posed and has radial derivative in terms of Bessel functions. Denote $\oint \frac{\partial}{\partial\rho}(\sum_i f_{i,j})|_{\rho\to R}\, d\phi$ by ξ, then

$$H(Z) = \mu_2^2 Z + C_1(0) - \frac{\xi\cdot\gamma}{1+VS'(1)} \int_0^{\infty} \left(\sum_{n=0}^{\infty} \sum_i \frac{A_{i,n}}{\lambda} \right) e^{-\lambda Z}\, d\lambda \tag{3.83}$$

To complete the boundary layer solution (3.46), Now consider the oxygen con-

centration φ in boundary tissue layer to the second order of ε. This solution can be written in terms of a new variable W as

$$\begin{aligned}\varphi(r,\theta,Z) &= W(r,Z) + \mu_2 Z^2 + r^2/4 + \sum_{j=1}^{N} C_{1,j}(0) \\ &\quad - \widehat{\xi} \int_0^\infty A(\lambda)\, e^{-\lambda Z}\, d\lambda \\ &\quad + \mu_2/2 \cdot \sum_{j=1}^{N} \ln[r^2 + a_j^2 - 2ra_j \cos(\theta - \alpha_j)] \\ &\quad - 2\mu_2 \sum_{n=0}^{\infty} r^n (A_n \cos n\theta + B_n \sin n\theta) \end{aligned} \tag{3.84}$$

where A_n, B_n are defined in (3.15) and (3.16), and

$$\widehat{\xi} = \frac{\xi \cdot \gamma}{1 + VS'(1)} \qquad \textit{and} \qquad A(\lambda) = \sum_{n=0}^{\infty} \sum_{i} \frac{A_{i,n}}{\lambda}$$

From Eqs. (3.55) to (3.58), $W(r,Z)$ satisfies

$$\frac{1}{r}\frac{\partial}{\partial r} r \frac{\partial W}{\partial r} + \frac{\partial^2 W}{\partial Z^2} = \widehat{\xi} \int_0^\infty \lambda^2 A(\lambda)\, e^{-\lambda Z}\, d\lambda \tag{3.85}$$

$$\frac{\partial W}{\partial r}\Big|_{r=1} = 0, \qquad Z \geq 0 \tag{3.86}$$

$$\frac{\partial W}{\partial Z}\Big|_{Z=0} = -\widehat{\xi} \int_0^\infty \lambda A(\lambda)\, d\lambda, \qquad r \leq 1 \tag{3.87}$$

Notice that W does not depend on θ. As Salathe and Wang [24] has shown in their paper, the capillary source concentration is already included in the rest of the expression for φ in (3.84) to the second order of ε as shown in (3.43). The solution to the poisson equation (3.85) with boundary condition (3.86) and (3.87) can be constructed by using eigenfunction expansions $g_n(r)$, in the form of

$$g_n(r) = Y_0(\lambda_n R) J_0(\lambda_n r) - J_0(\lambda_n R) Y_0(\lambda_n r) \tag{3.88}$$

where J_0 and Y_0 are the zero order bessel functions of the first and second kind. the eigenvalues λ_n are obtained from boundary condition (3.86) the roots of

$$Y_0(\lambda R)\, J_1(\lambda) \; - \; J_0(\lambda R)\, Y_1(\lambda) \; = \; 0 \tag{3.89}$$

where J_1 and Y_1 are the first order bessel functions of the first and second kind. A solution to Eq. (3.85) with boundary conditions (3.86) and (3.87) can be found (Salate and Wang [24])by constructing $W(r, Z)$ in the form

$$W(r, Z) \; = \sum_{n}^{\infty} E_n(Z) g_n(r) \tag{3.90}$$

where $E_n(Z)$ is a more general function of Z instead of $e^{-\lambda Z}$ and $g_n(r)$ are eigenfunctions associated with the equation for r after separation of variables, defined in (3.89). The orthogonality property of the eigenfunctions gives

$$\oint r g_m(r) g_n(r) dr \; = \; 0, \quad for \quad m \neq n \tag{3.91}$$

$$\oint r g_n^2(r) dr \; = \; \frac{\Big(g_n(1)\Big)^2}{2} \; - \; \frac{2}{\lambda_n^2 \pi^2}, \quad n = 1, 2, 3, 4... \tag{3.92}$$

After applying Eqs (3.91) and (3.92) to relation (3.90) using the orthogonality property and multiplying $g_m(r)$ on both sides of (3.90), one can conclude that

$$E_n(Z) \; = \; P_n \cdot \oint r W(r, Z) g_n(r) dr \tag{3.93}$$

with

$$P_n \; = \; \left[\frac{\Big(g_n(1)\Big)^2}{2} \; - \; \frac{2}{\lambda_n^2 \pi^2} \right]^{-1} \tag{3.94}$$

Differentiating E_n twice with respect to Z gives

$$E_n''(Z) = P_n \cdot \oint r\, g_n(r) \frac{\partial^2 W(r,Z)}{\partial Z^2} dr \tag{3.95}$$

together with the governing Eq. (3.85), it yields

$$\begin{aligned} E_n''(Z) = -P_n \cdot \oint g_n(r) \frac{\partial}{\partial r} r \frac{\partial}{\partial r} W(r,Z) dr \\ + P_n \left(\widehat{\xi} \int_0^\infty \lambda^2 A(\lambda)\, e^{-\lambda Z}\, d\lambda \right) \cdot \oint r g_n(r) dr \end{aligned} \tag{3.96}$$

By using the boundary conditions for W, applying integration by parts twice and using the Eq. (3.93), the first integral on the right side of Eq. (3.96) is reduced to

$$\begin{aligned} \oint g_n(r) \frac{\partial}{\partial r} r \frac{\partial}{\partial r} W(r,Z) dr &= -\lambda_n^2 \oint r W(r,Z) g_n(r) dr \\ &= -\lambda_n^2 P_n^{-1} E_n \end{aligned} \tag{3.97}$$

The second integral on the right side of Eq. (3.96) using properties for Bessel functions (Watson [26]) can be reduced to

$$\oint r g_n(r) dr = -\frac{2}{\lambda_n^2 \pi} \tag{3.98}$$

Therefore, combining (3.96), (3.97) and (3.98) it gives

$$E_n''(Z) = \lambda^2 E_n(Z) - \frac{2\widehat{\xi} P_n}{\lambda_n^2 \pi} \int_0^\infty \lambda^2 A(\lambda)\, e^{-\lambda Z}\, d\lambda \tag{3.99}$$

From property (3.93) and the boundary condition (3.87), another boundary condition for $E_n(Z)$ is obtained

$$E_n'(0) = \frac{2\widehat{\xi} P_n}{\lambda_n^2 \pi} \int_0^\infty \lambda A(\lambda)\, d\lambda \tag{3.100}$$

General solutions to Eq. (3.99) can be achieved given the boundary condition (3.100)

The solution in cylindrical tissue c and the solution in capillaries C are computed outside the boundary layer where z is comparably small, as well as the other end boundary layer, which form the two end regions of our cylindrical model. The solutions obtained in the middle intermediate region are valid through the cylindrical tube except for the two end regions. For the arterial boundary layer, one can use perturbation method by letting $Z = z/\varepsilon$ to find the approximate solutions $\widetilde{C}$ and $\widetilde{c}$ suggested as shown above to the first and second order of ε. Similarly for the venous end region by letting $Y = (1 - z)/\varepsilon$ one can approach the solutions with respect to the first and second order of ε as well. A single solution shall be constructed through the whole cylindrical region from $z = 0$ to $z = 1$ uniformly composed from the outer solutions C, c from section 1 and the inner solutions $\widehat{C}$, $\widehat{c}$ from section 2. This can be done by adding the outer solutions and inner solutions for both the arterial and venous boundary layers, and subtracting the common terms from the expansions.

$$C_{uniform} = C + \widetilde{C} - C_{common}$$

$$c_{uniform} = c + \widetilde{c} - c_{common}$$

The common solutions are needed in order to find the uniform solutions for capillary and tissue oxygen concentration. Observe the oxygen concentration in capillaries given in central region as approximated by (3.42) and in small z boundary layer region as given by (3.45). It gives

$$C_{comm} = 1 + \varepsilon\,\mu_1 Z + \varepsilon^2\Big(\mu_2 Z^2 + C_1(0)\Big) \tag{3.101}$$

Observe the oxygen concentration in tissue given in central region as approximated

by (3.43) and in arterial boundary layer region as given by (3.46). It gives

$$\begin{aligned} c_{comm} &= N + r^2/4 - \kappa/4 \cdot \sum_{j=1}^{N} \ln[r^2 + a_j^2 - 2ra_j \cos(\theta - \alpha_j)] \\ &\quad + \kappa \sum_{n=0}^{\infty} r^n (A_n \cos n\theta + B_n \sin n\theta) + \varepsilon \sum_{j=1}^{N} \mu_{1,j} Z \\ &\quad + \varepsilon^2 \Big\{ \mu_2 Z^2 + r^2/4 + \sum_{j=1}^{N} C_{1,j}(0) \\ &\quad + \mu_2/2 \cdot \sum_{j=1}^{N} \ln[r^2 + a_j^2 - 2ra_j \cos(\theta - \alpha_j)] \\ &\quad - 2\mu_2 \sum_{n=0}^{\infty} r^n (A_n \cos n\theta + B_n \sin n\theta) \Big\} \end{aligned} \tag{3.102}$$

Therefore the uniformly composite solution for the capillary oxygen concentration through the central region and the small z boundary layer is given from (3.7) and above

$$C_{ucs} = C_0(z) + \varepsilon^2 C_1(z) + (\widetilde{C} - C_{comm}) \tag{3.103}$$

where

$$\widetilde{C} - C_{comm} = \varepsilon^2 \cdot \left\{ - \frac{\xi \cdot \gamma}{1 + VS'(1)} \int_0^{\infty} \left(\sum_{n=0}^{\infty} \sum_i \frac{A_{i,n}}{\lambda} \right) e^{-\lambda Z} \, d\lambda \right\} \tag{3.104}$$

So then from Eqs. (3.103) and (3.104), it gives

$$\begin{aligned} C_{ucs} &= C_0(z) + \varepsilon^2 \Big\{ C_1(z) \\ &\quad - \frac{\xi \cdot \gamma}{1 + VS'(1)} \int_0^{\infty} \left(\sum_{n=0}^{\infty} \sum_i \frac{A_{i,n}}{\lambda} \right) e^{-\lambda Z} \, d\lambda \Big\} \end{aligned} \tag{3.105}$$

This solution is valid throughout both of the central region and the arterial boundary layer region, for the last term of Eq. (1.105) vanishes as Z goes arbitrarily large,

meaning that the dominant effect is given by $C_0 + \varepsilon^2 C_1$ which gives exactly the solutions for oxygen in capillary through the central region.

For the uniform composite solution of the tissue oxygen concentration through the central region and the arterial boundary layer. Similarly from (3.7) and (3.102) it is given as

$$c_{ucs}(r, \theta, z) = c_0(r, \theta, z) + \varepsilon^2 c_1 + (\widetilde{c} - c_{comm}) \tag{3.106}$$

This solution is valid throughout both of the central region and the arterial boundary layer region. The dominant effect is given by $c_0 + \varepsilon^2 c_1$ and solutions of oxygen concentration can be unified through the mixed layer near the end of tissue cylinder.

In conclusion, axial diffusion can be neglected for long and parallel capillaries. However, it may play an important role in oxygen transportation in tissue specially when a relatively short pathway is counted into one's consideration. Analytical solution for rectangular and circular regions are given and one can extend the discussion of effect of axial diffusion onto a cuboid capillary domain. For irregular shaped domains, numerical implement is necessary for analyzing oxygen distribution across the region. A compartmental numerical model is introduced in the next chapter.

Chapter 4

A Compartmental Model of Multi-Capillary Supply Region

4.1 The Basic Problem

Consider a cross-sectional region perfused with N parallel capillaries at arbitrary locations and arbitrary diffusion fluxes q_i $(1 \leq i \leq N)$. The axial variation is small and can be neglected. The diffusion-consumption equation suffices

$$\nabla^2 C = 1 \tag{4.1}$$

where $C = C_u/C_A$ is the normalized with respect to oxygen concentration of the arterial blood, C_A. The oxygen consumption κ_0 in the surrounding tissue to the zeroth order, can be normalized by a nonhomogeneous term 1, and is equal to the sum of the fluxes out of the capillaries. It was found by Wang([12]) that due to uneven capillary characteristics, the capillary domains are highly contorted, differ from either the Krogh circular cylinder or Voronoi polygonal cylinders.

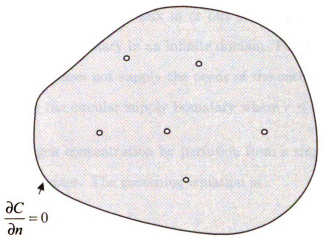

Figure 4.1: Arbitrary multi-capillaries in a cross-sectional tissue region

For uneven consumption rate, we can write

$$\nabla^2 C = \kappa(x, y) \tag{4.2}$$

where $\kappa(x, y)$ is the consumption rate at (x, y) and satisfies

$$\frac{\int\int \kappa(x, y) dx dy}{\int\int dx dy} = 1 = \sum_{1}^{N} q_i \tag{4.3}$$

The solution to such nonhomogeneous problem is still possible, using Green's functions. But in practice $\kappa(x, y)$ is unknown, usually related to the capillary strengths q_i. For example, when one capillary of a well perfused region is experiencing obstruction, and the rest of the capillaries could not react in time, the delivery (and consumption) of the region in the neighborhood of the obstructed capillary would decrease, but we do not know where and how much.

One reasonable model of the oxygen consumption of tissue is the all-or-none model. Each location of the tissue is ether fully supplied or completely ischemic. To illustrate

this model, noticing that in previous two chapters we discussed the case for insulated rectangular or circular regions with no flux in or out of the domain, we start first here with the case of a single capillary in an infinite domain. For unbounded domain with one single capillary, it does not supply the needs of the entire tissue area. The region is ischemic outside the circular supply boundary where $r \leq R$.

Let C denote the oxygen concentration by perfusion from a single capillary with oxygen strength q at the center. The governing equation is

$$\nabla^2 C = 1 \qquad r \leq R \tag{4.4}$$

and the oxygen flux is zero at $r = R$

$$C = \frac{\partial C}{\partial r} = 0, \qquad at \qquad r = R \tag{4.5}$$

$$\lim_{r=0} (-2r \frac{\partial C}{\partial r}) = q \tag{4.6}$$

The solution to Eqs (3.4) and (3.6) is

$$C = \frac{r^2}{4} - \frac{q}{2} \ln r + p \tag{4.7}$$

where the constants R and p are found by Eq.(3.5)

$$R = \sqrt{q}, \qquad p = \frac{q}{4}(\ln q - 1) \tag{4.8}$$

The oxygen concentration decreases from the center of the source through the tissue area to the boundary at $\sqrt{q}$. This region inclosed by the circular boundary is also referred as the capillary supply region. Fig. (4.2) shows the result.

The all-or-none model is reflected by myocardial infarction where necrotic regions

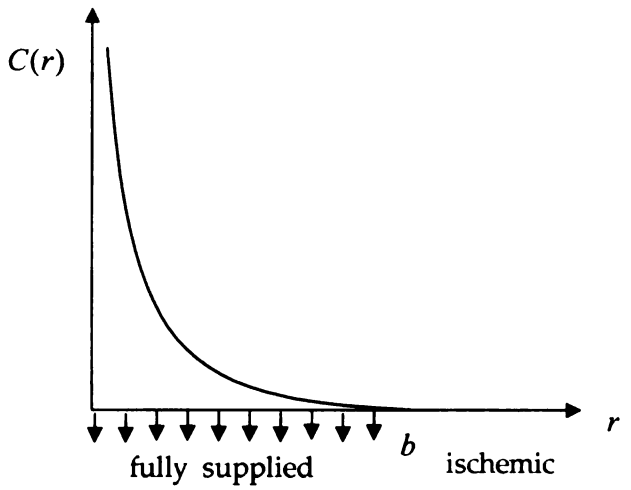

Figure 4.2: Oxygen supplied and ischemic regions as result from Eq. (4.4)

are clearly demarcated. In contrary the first order consumption model

$$\nabla^2 C = \alpha C \tag{4.9}$$

or the Michaelis-Menten model

$$\nabla^2 C = \frac{\alpha C}{\beta + C} \tag{4.10}$$

would give solutions which yield non-zero concentration effects at $r- > \infty$, which does not happen in reality.

However if there are more than one capillary, the problem becomes very difficult since the boundary of the ischemic area is no longer circular and is not known a priori. The question is similar to the blockage of one capillary in Fig (4.3), where we have an ischemic area of unknown boundary. This area may be decreased by an increase in flux from the neighboring perfused capillaries. But such adjustments would unlikely be immediate.

The mathematical problem now become difficult due to the unknown boundary

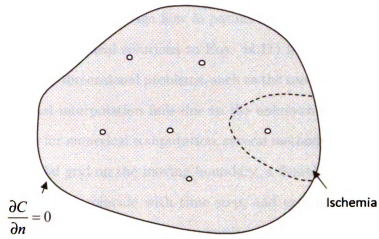

Figure 4.3: Blockage of one single capillary

location. Our method is to approach the steady-state by a transient process, which paradoxically may be more efficient than the steady state problem.

4.2 Unsteady Diffusion-Consumption

The unsteady equation for concentration is

$$\frac{\partial C}{\partial t} = \nabla^2 C - \kappa(x, y, t) \tag{4.11}$$

where

$$\kappa(x, y, t) \tag{4.12}$$

The boundary of the perfused region $p(x, y, t) = 0$ is unknown. On this boundary

$$p(x, y, t) = \frac{\partial C}{\partial n}(x, y, z) = 0 \tag{4.13}$$

where n is the normal to the boundary. The problem is a difficult moving boundary

problem or known as Stefan problem (Crank[28]), studied in the context of freezing and melting of materials and seepage flow in porous media.

There exist some analytical solutions to Eqs. (4.11) in one dimension including axisymmetric. For two dimensional problems, such as the case for multiple capillaries, even direct numerical interpolation fails due to the unknown moving boundary. To locate the boundary for numerical computation, several methods are suggested. These include fixing a partial grid on the moving boundary, a flexible grid that include the boundary, grid lines that coincide with time step, and exchange of dependent and independent variables. All are impossible to implement in two dimensions.

The 2D ischemic quasi-steady problem was attempted by Salathe and Wang [23] using a Krogh cylinder and a perturbation from steady. The best method to treat truly 2D unsteady problem with moving boundary is the truncation scheme proposed by Berger, Ciment and Rogers [3]. They used a large, fixed domain, and set or truncate any negative values of concentration to zero. Since the domain is fixed, the usual finite difference numerical schemes can be used. The moving front is then the zero concentration curve. The method is applied to a 2D oxygen diffusion problem by Evans and Gourlay [54] who used a hopscotch finite difference method to increase stability.

In what follows we shall propose a compartmental diffusion consumption model which is much simpler than the truncation-finite difference method of Berger et al([3]).

4.3 Essence of the Compartmental Model

Consider the whole plane partitioned into contiguous finite tissue bins. Each bin would consume one unit of oxygen per unit of time, if sufficient oxygen supply is available. If oxygen is less than the amount to fully suffice the plane, the bin is hypoxic and therefore consumes all available oxygen. Some of the bins are designated as capillaries which produce relatively large amount of oxygen per unit of time. By Fick

diffusion law through membrane separations, those bins with high substrate/oxygen concentration would diffuse into adjacent bins where substrate/oxygen concentration is low. Within each bin the oxygen content is even or well mixed. Therefore the whole system is a network of physical compartments. The resulting equations are similar to the discretized diffusion - consumption equations but are formulated from completely different principles.

First let us look at some examples in 1D.

I. 1D Unsteady Diffusion

Consider the one dmensional problem $C(x,t)$, $x \geq 0$, where the concentration at $x = 0$ when $t = 0$ is suddenly raised and kept at a normalized value of 1. The governing equation is

$$\frac{\partial C}{\partial t} = \frac{\partial^2 C}{\partial x^2} \tag{4.14}$$

with the boundary and initial conditions

$$C(0,t) = 1, \qquad C(\infty,t) = 0 \tag{4.15}$$

$$C(x,0) = 0, \qquad x > 0 \tag{4.16}$$

We shall compare it with the exact solution

$$C(x,t) = erfc(\frac{x}{2\sqrt{t}}) \tag{4.17}$$

where $erfc$ is the complementary error function. (Crank 1975)

Instead of the partial differential equations approach, consider a domain $x \geq 0$ which is composed of ordered compartments of width δx in 1D,

The i^{th} compartment is between $(i-1)\Delta x$ and $i\Delta x$. Each compartment exchanges oxygen with adjacent compartments through Fick diffusion law. Let C_i be

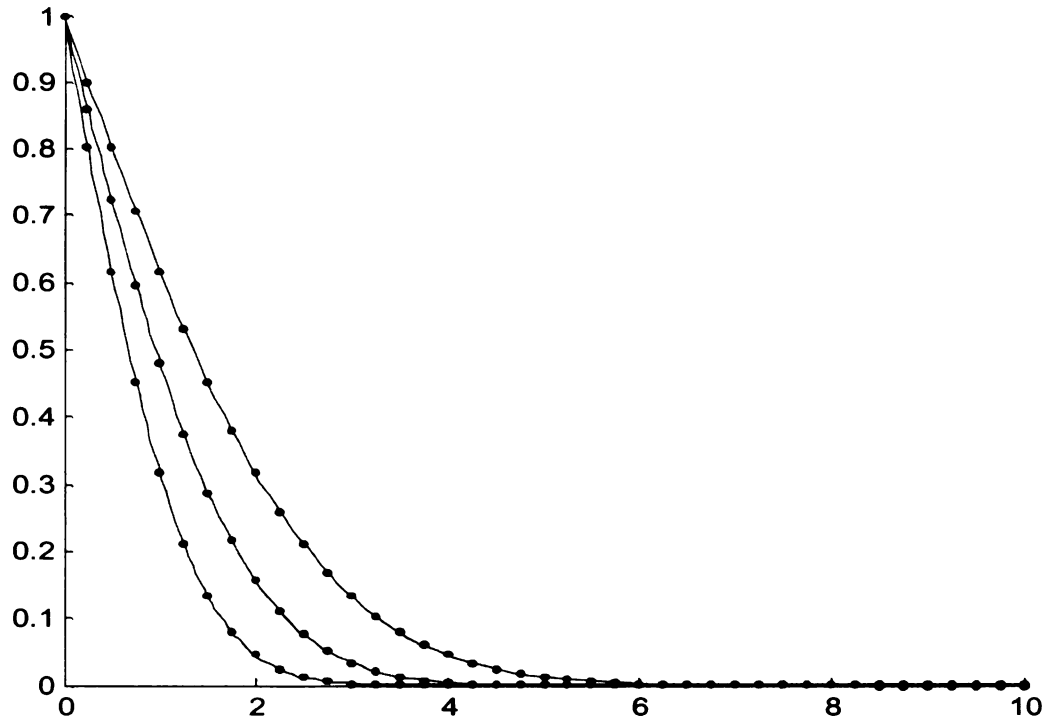

Figure 4.4: Result compared with solutions from Eq. (4.17) at t=0.5, t=1 and t=2

tration distributions from Eq. (4.21) at $t = n \cdot \Delta t$. Fig (4.4) shows the result for $\Delta x = 0.1$, $\alpha = 0.1$. We see that the dots computed from Eq. (4.21) coincides with the curve generated by the exact solution Eq. (4.17).

II. 1D Unsteady Diffsion-Consumption

Let Ω be the perfused region of tissue. The governing equation is

$$\frac{\partial C}{\partial t} = \frac{\partial^2 C}{\partial x^2} - 1, \qquad x \in \Omega \tag{4.23}$$

with the boundary and initial conditions

$$\frac{\partial C}{\partial x} = C = 0 \qquad \text{on the boundary at} x = b \tag{4.24}$$

$$C(0,t) = 1, \tag{4.25}$$

the concentration of the i^{th} compartment. Thus

$$\Lambda\Delta x\frac{dC_i}{t} = k\Lambda(C_i - C_i) + k\Lambda(C_{i+1} - C_i) \tag{4.18}$$

where Λ is the area of diffusion and k is the transfer coefficient. Eq (4.18) can be rewritten as

$$\frac{dC_i}{t} = k\Delta x\left[\frac{C_{i-1} - 2C_i + C_{i+1}}{(\Delta x)^2}\right] \tag{4.19}$$

In the limit of $\Delta x \to 0$ we see the last bracket is $\partial^2 C/\partial x^2$, thus $(k\Delta x)$ must be the diffusivity which we have normalized to unity in Eq. (4.14)

Now consider very small time step Δt

$$t = \Delta t \cdot n \tag{4.20}$$

and replace dC_i/dt by $(C_{i,n+1} - C_{i,n})/\Delta t$ where n denotes the time. Eq. (4.19) now becomes the algebraic equation

$$C_{i,n+1} = C_{i,n} + \alpha \cdot (C_{i-1,n} - 2C_{i,n} + C_{i+1,n}) \tag{4.21}$$

where $\alpha = \Delta t/(\Delta x)^2$ which is in the order of $o(1)$. This is exactly the finite difference explicit discretization of Eq. (4.14) (Mitchell, 1964)

In the beginning, all compartments are empty except the concentration of the zeroth compartment is maintained at 1.

$$C_i = \begin{cases} 0 & i \neq 0 \\ 1 & i = 1 \end{cases} \tag{4.22}$$

Also $C_{0,n} = 1$, all n

For given $\alpha \ll 1$ and Δx, get $\Delta t = \alpha(\Delta x)^2$, we generate subsequent concen-

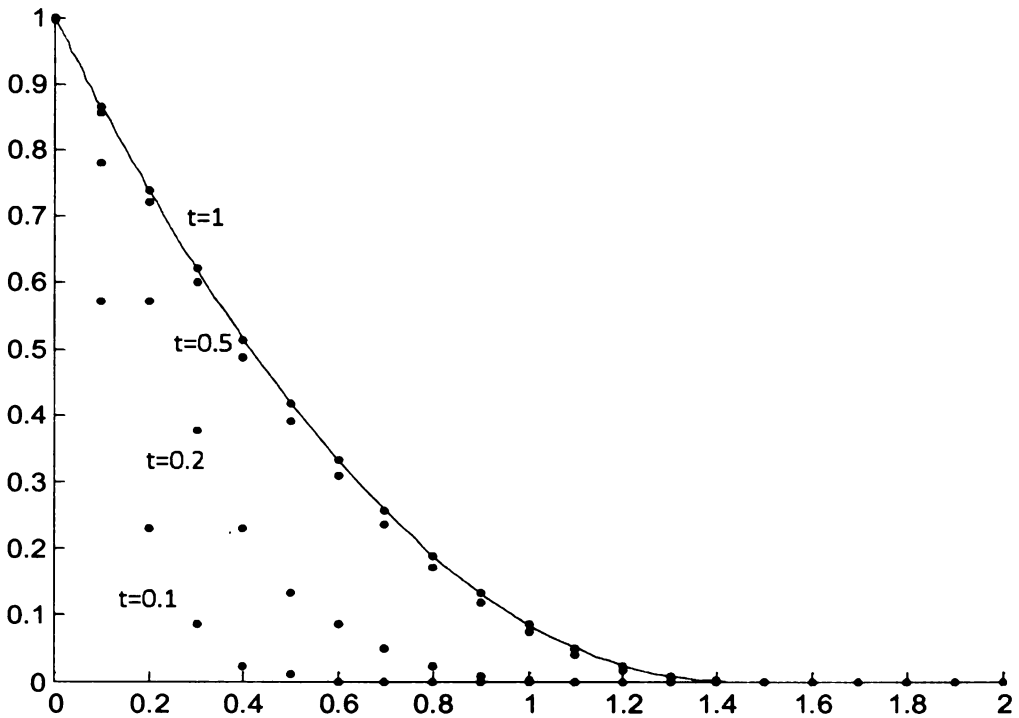

Figure 4.5: Oxygen diffusion into a consuming region at t=0.1, t=0.2, t=0.5, t=1

$$C(x,0) = \begin{cases} 0 & x \neq 0 \\ 1 & x = 0 \end{cases} \tag{4.26}$$

The solution for the final steady state is

$$C = \frac{x^2}{2} - \sqrt{2}x + 1, \qquad t \to \infty \tag{4.27}$$

As shown in section (4.1), the region $0 \leq x \leq \sqrt{2}$ is fully perfused, elsewhere ischemic. We shall use the compartmental method on the transient problem. Balancing mass on the ith compartment, we obtain

$$\Lambda \Delta x \frac{dC_i}{t} = k\Lambda(C_i - C_i) + k\Lambda(C_{i+1} - C_i) - \Lambda\Delta x \tag{4.28}$$

where Λ is the area of diffusion and k is the transfer coefficient. Thus

$$C_{i,n+1} = C_{i,n} + \alpha \cdot (C_{i-1,n} - 2C_{i,n} + C_{i+1,n}) - \Delta t \tag{4.29}$$

If $C_{i,n+1}$ is found to be negative, it is set to be zero and the compartment is labeled ischemic. Fig. (4.5) shows the spread of the oxygen diffusion from a plane into a consuming region. Note when $t = 1$ the computed results have reached the steady state exact solution in Eq. (4.27).

For stability, similar to finite difference explicit methods, α shall be less than 0.5. Otherwise implicit or semi-implicit schemes would improve stability but introduce systems of equations to be solved.

4.4 2D Compartmental Model

For one dimensional unsteady diffusion, the compartmental model leads to similar equations as the finite difference method. For 2D, the compartmental model has decisive advantages.

Hexagonal compartments are utilized to cover the whole tissue region. Firstly, the compartmental model is quite simple to implement. In comparison, the 2D unsteady finite difference schemes are quite complicated. Secondly, finite differences are normally used in a square grid, while the compartments used here can be of any shape. i.e. one can use tissue cell boundaries or Voronoi domains like shown in Fig 1.1. Here we shall use hexagonal compartments which are more natural than squares.

Notice in Fig (4.6 a)) the spread of a square grid, having only four neighbors, is more distorted or uneven than the spread of a hexagonal grid which has six neighbors. The neighbors of the (i,j)th cell are

$$(i-1,j+1),\ (i,j+1),\ (i-1,j),\ (i+1,j),\ (i,j-1),\ (i+1,j-1) \tag{4.30}$$

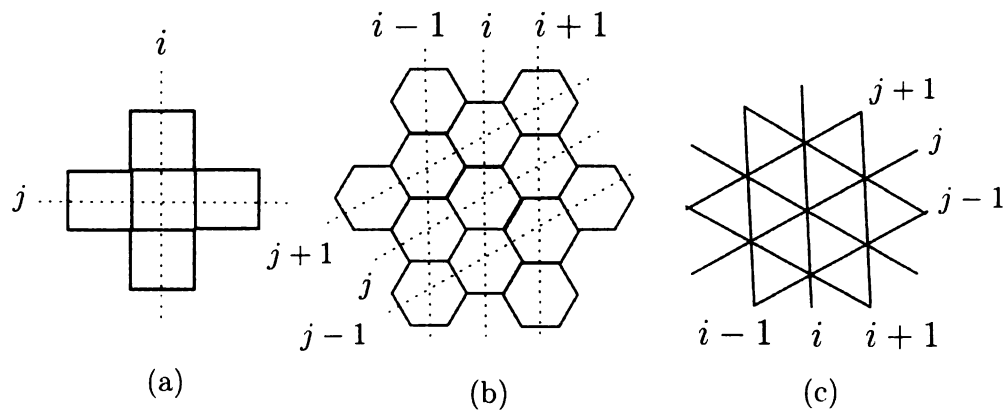

Figure 4.6: Compartments of a) square b) hexagonal c) triangular

Now consider the (i, j) cell of area Λ, height h with side length l.

$$l = \frac{2\Delta x}{3} \tag{4.31}$$

$$\Lambda = \frac{2(\Delta x)^2}{\sqrt{3}} \tag{4.32}$$

Mass balance gives

$$\begin{aligned} \Lambda h \frac{dC_{ij}}{dt} &= \kappa l h \cdot (C_{i-1,j+1} + C_{i,j+1} + C_{i-1,j} + C_{i+1,j} \\ &\quad + C_{i,j-1} + C_{i+1,j+1} - 6C_{ij}) \\ &\quad - \kappa \Lambda h \end{aligned} \tag{4.33}$$

Here C_{ij} is the concentration of the (i, j)th cell, κ is the transfer coefficient, or permeability through the cell boundary, and κ is the consumption as in mass per volume per time. Comparing the above with the diffusion equation

$$\begin{aligned} \frac{\partial C}{\partial t} &= D\left(\frac{\partial^2 C}{\partial x^2} + \frac{\partial^2 C}{\partial y^2}\right) - \kappa \\ &= D\left(\frac{C_{i,j+1} + C_{i+1,j} + C_{i-1,j} + C_{i,j-1} - 4C_{ij}}{(\Delta x)^2}\right) - \kappa \end{aligned} \tag{4.34}$$

we find diffusivity

$$D = \frac{\kappa l}{\Lambda} \cdot \frac{6}{4}(\Delta x)^2 = \frac{\kappa(\Delta x)}{2\sqrt{3}} \tag{4.35}$$

Normalize all lengths by R which is a measure of the size of the region, the concentration by $\kappa R^2/D$ and the time by R^2/D, Eq. (4.33) becomes

$$\frac{dC_{ij}}{dt} == \frac{2}{3}\left(\frac{\sum neighbors - 6C_{ij}}{(\Delta x)^2}\right) - 1 \tag{4.36}$$

To discretize the time using explicit method, If time is discretized by $t = n \cdot \Delta t$

$$C_{i,j,n+1} = C_{i,j,n} + \alpha(\sum neighbors - 6C_{i,j,n}) - \Delta t \tag{4.37}$$

here $\alpha = 2\Delta t/3(\Delta x)^2$ and

$$\sum neighbors = C_{i-1,j+1} + C_{i,j+1} + C_{i-1,j} + C_{i+1,j} + C_{i,j-1} + C_{i+1,j+1} \tag{4.38}$$

The coordinates (x, y) are related to (i, j) by

$$\begin{aligned} x &= i\,\Delta x \\ y &= (j + \frac{i}{2})\frac{2}{\sqrt{3}}\,\Delta x \end{aligned} \tag{4.39}$$

For this free boundary problem, one can choose a large region which contains the oxygen well sufficed and consumed area. For example, if the outer boundary is not oxygenated, we can use a rhombic region where $i = -N, N$, $j = -N, N$ large enough to contain any perfused regions. On the rhombic boundary, one can prescribe $C = 0$ which is equivalent to the zero flux condition $\partial C/\partial n = 0$. In the case the zero flux condition is truly needed, the concentrations of adjacent cells in the normal direction

can be prescribed equal. For example alone $j = -N$

$$C_{i,-N+1} = C_{i,-N} \tag{4.40}$$

or even better, remove the two outside neighboring bins $C_{i,-N}$, $C_{i+1,-N}$. Similarly for $i = -N$ one can use

$$C_{-N+1,j} = \frac{1}{2}\left(C_{-N,j} + C_{-N,j+1}\right) \tag{4.41}$$

or remove the two neighboring bins $C_{-N,j}$, $C_{-N,j+1}$.

Similar relations can be obtained for Dirichlet boundary conditions $y = constant$ or any curved boundary.

Now consider one of the cell is a capillary or oxygen source. Suppose the flux is Q, nourishing a region of πr^2 in the steady state. This region contains $\pi r^2/\Lambda - 1$ consuming cells. If each cell consumes one unit of substrate per time, the total flux needed from the capillary is

$$Q = \left(\frac{\pi r^2}{\Lambda} - 1\right) \cdot 1 \tag{4.42}$$

Let $r = J\,\Delta x$, then from Eq. (4.34)

$$Q = \left(\frac{\pi\sqrt{3}}{2} J^2 - 1\right) \tag{4.43}$$

For a radius of $r = 1, \Delta x = .1$, $Q = 271$, a radius of .5, $Q = 67$. Now by Fick diffusion law, the oxygen flux is evenly distributed through the membranae wall between each two adjacent cells, therefore $Q/6$ amount of oxygen is supplied to each of the capillary neighboring cells in time of Δt. The governing equation of oxygen

concentration for capillary neighboring compartments (i, j) is

$$C_{i,j,n+1} = C_{i,j,n} + \alpha\,(\sum^{5cells} neighbors - 5C_{i,j,n}) + \frac{Q}{6}\Delta t - \Delta t \tag{4.44}$$

4.5 Examples and Discussion

First, we look at the case with one single capillary in the center with flux strength sufficiently enough for a circular supply region with radius $r = 1$. From the results shown in previous section, as $t \to \infty$ the concentration profile should approach

$$C = \frac{r^2}{4} - \frac{1}{2}\ln r - \frac{1}{4} \tag{4.45}$$

which is from the steady state solution for Eq. (4.7). Here we use $\alpha = 0.1$,$\Delta x = 0.01$ and $tt = 0.5$. We display the results as in Fig. (4.7) to (4.9) which shows the oxygen concentration profiles at $t = 0.01$, $t = 0.1$ and $t = 1$.

When time is small, the spread is approximately hexagonal, showing the effect of the grid. For larger time the spread becomes circular. Table (4.1) shows the radius of the supply region against time. At $t = 0.5$ the radius reaches 0.972 which is close the steady state estimate of 1. Fig (4.10) shows the radial oxygen distribution error as results compared with Eq. (4.45). As the compartment partition becomes smaller, we can adjust the size of our capillary source by adding a fixed number of compartments so that the capillary wall is approximated by the outer region of the source compartment boundary.

	$t = 0.01$	$t = 0.05$	$t = 0.1$	$t = 0.5$	$t = 1$
r	0.124	0.699	0.817	0.972	0.996

Table 4.1: Radius of the circular supply region

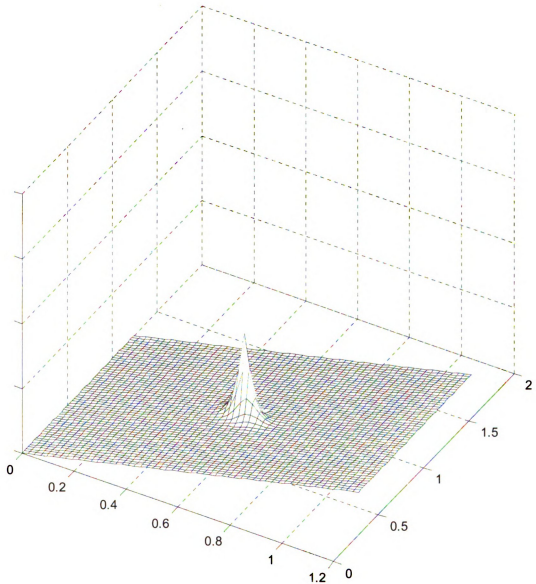

Figure 4.7: Oxygen concentration profile with one single centered capillary at $t = 0.01$

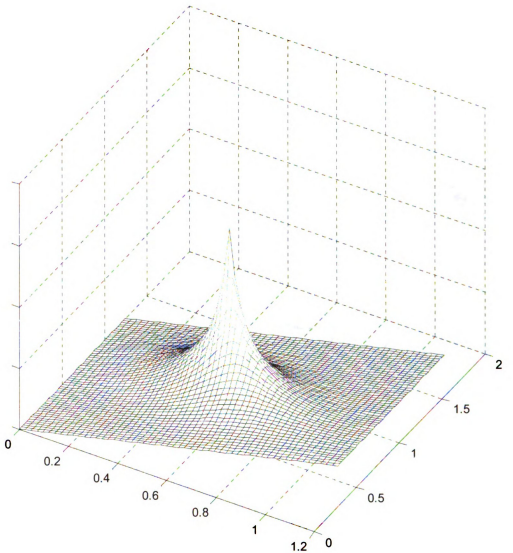

Figure 4.8: Oxygen concentration profile with one single centered capillary at $t = 0.1$

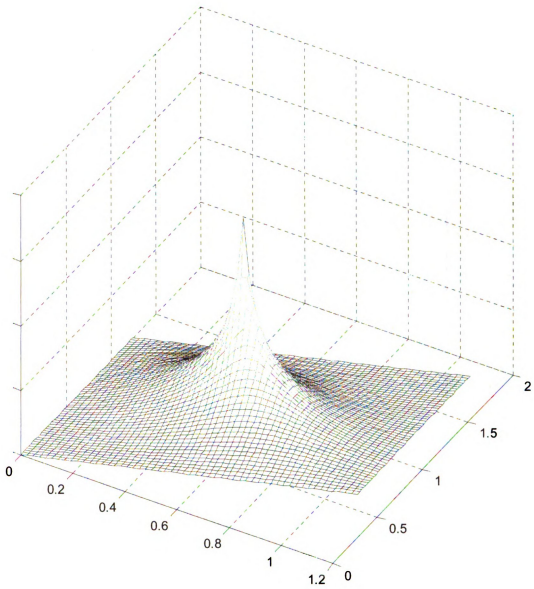

Figure 4.9: Oxygen concentration profile with one single centered capillary at $t = 1$

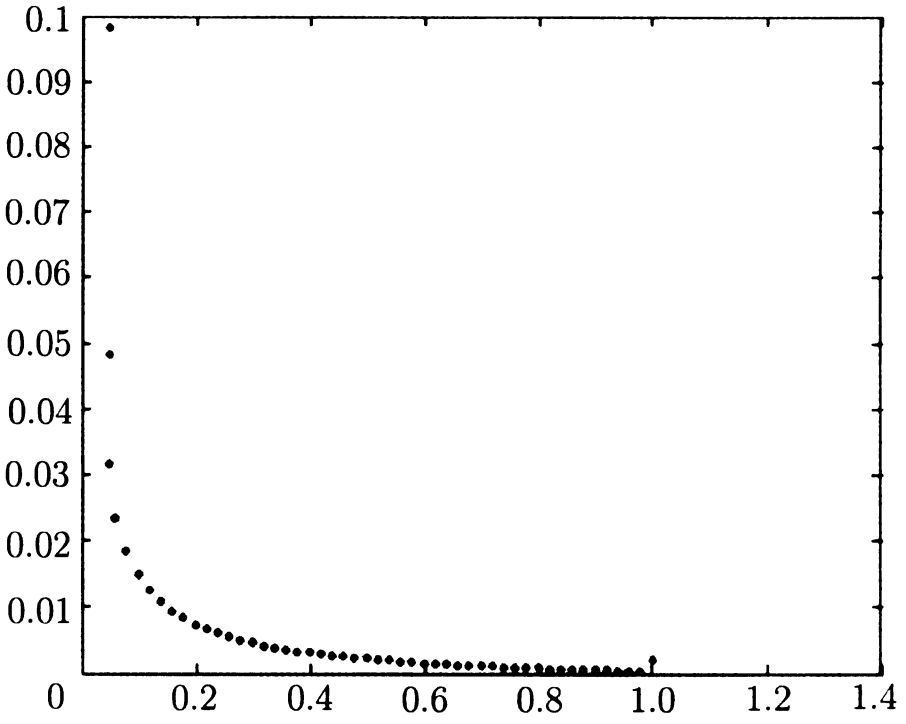

Figure 4.10: Radial oxygen concentration distribution error as results from example 1 compared to Eq. (4.45)

Using the compartmental model, we can construct boundaries with different shapes as well as for studying insulated closed regions. Due to the natural properties of hexagonal boundaries, the insulated region boundary can be of hexagonal or rhombic. We can also illustrate the oxygen concentration in its transient state using an approximated rectangular region.

Fig. (4.11) shows a schematic rectangular region bounded by $i = I$, $j = 2I - 1$, $j = 2(i - I) - 1$ and $i = i - I$. There are $2I^2 - 2I + 1$ cells in Fig. (4.11), $I = 4$ with 25 cells. The interior cells all have 6 neighbors. The boundary cells have less neighbors due to insulation from outside. There are four type of boundary cells. I. The four corner cells each has 2 neighbors, II. x boundary cells each has 4 neighbors, III. y outer boundary cells each has 3 neighbors, and IV. y inner boundary cells each has 5 neighbors. We can treat these cells differently applying the governing equation from Eq. (4.37) and make flux zero on each boundary cell walls.

Note that for Neumann boundary conditions such as the fully perfused insulated region, the steady concentrations are unique up to an additive constant, while for Dirichlet or mixed boundary conditions, such as partially ischemic cases, the steady concentrations are unique. This means the concentrations are independent of history, or how steady state is achieved.

	$dx = 0.2$	$dx = 0.1$	$dx = 0.01$	$dx = 0.004$	$dx = 0.001$
Number of cells	41	181	19801	124501	1998001
Cells of type II	6	16	196	496	1996
Cells of type III	6	16	196	496	1996
Cells of type IV	8	18	198	498	1998
Strength Q	67	217	2.72×10^4	1.7×10^5	2.72×10^6

Table 4.2: Parameters for compartmental model with different choices of dx

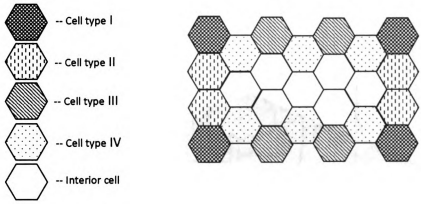

Figure 4.11: Schematic regular supply region with $I = 4$

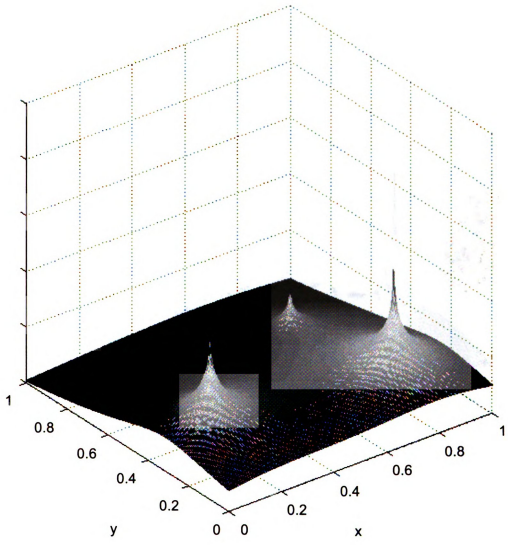

Figure 4.12: Oxygen concentration profile at $t = 0.1$, numerical results shown in an insulated capillary-tissue region

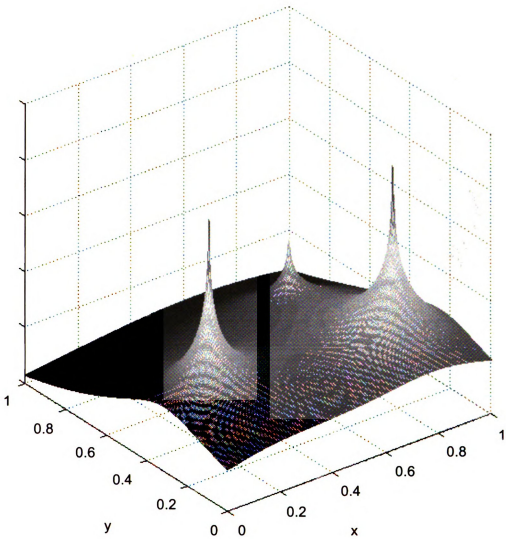

Figure 4.13: Oxygen concentration profile at $t = 1$, numerical results shown in an insulated capillary-tissue region

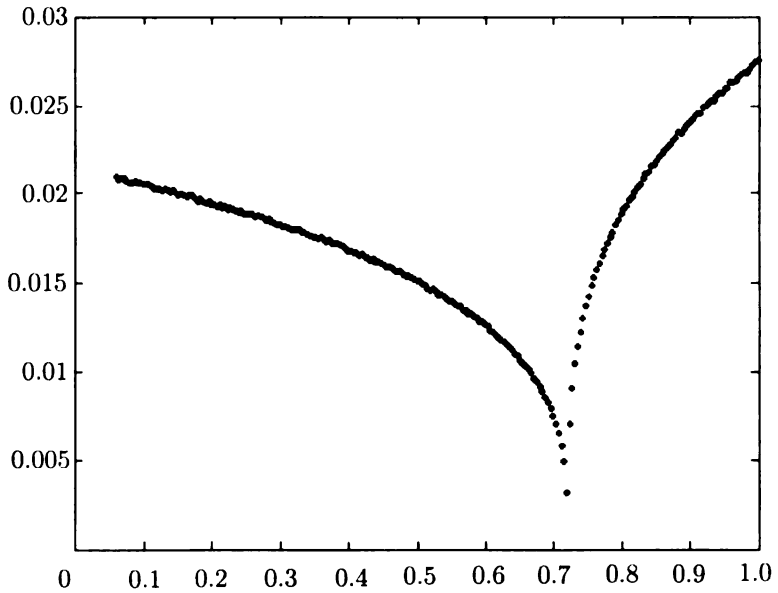

(a)

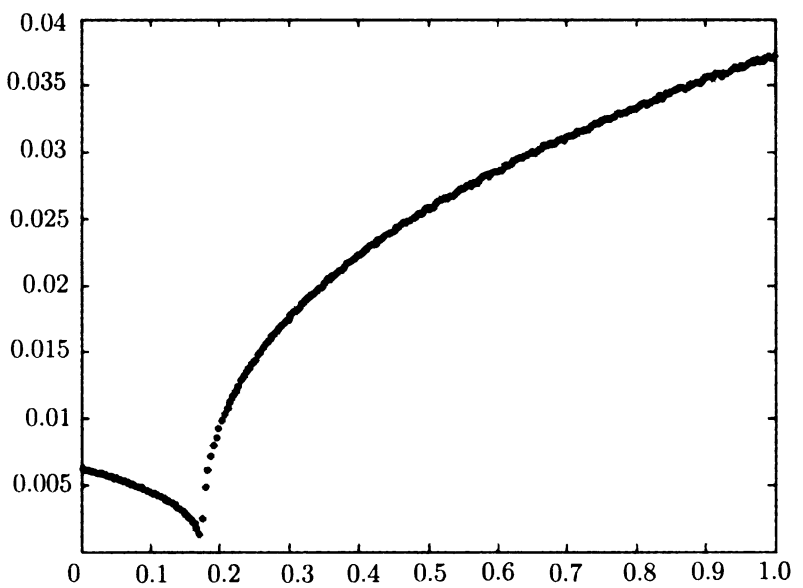

(b)

Figure 4.14: oxygen concentration ratio comparison with Example II in Chapter two a) Normalized concentration comparison at source one where $y = 0.821$ b) Normalized concentration comparison at source two where $x = 0.243$ Errors are relative low at each source point

For multiple capillaries with insulated region. Using the source locations from Example II in Chapter two, we approximate the rectangular region by the hexagonal compartmental model. The following sources are given in table (2.6). Use $dx = 0.004$, $\alpha = 0.1$. The total flux strength from three capillaries are calculated to satisfy the metabolic needs of the whole rectangular region. Fig. (4.12) and (4.13) shows the oxygen concentration at $t = 0.5$ and $t = 3.5$ respectively. The difference between the profiles at $t = 3.5$ and $t = 4$ is very small and we assume a steady state of is well achieved. Fig. (4.14) shows the oxygen concentration comparison between the compartmental model and the analytical results presented in example II of chapter two. Minimum oxygen concentration can be obtained on the boundary using the exact solution provided in chapter two. The two results differ by a constant, and this constant can be eliminated from consideration due to Neumann type of the boundary conditions.

One can, from the concentration distribution, determine the capillary domains of each source. The method is to find local minimums along the three grid lines i =const, j =const and $i + j$ =const. The boundary of the capillary domains must contain three local minimums. However, due to the approximate nature of the course grid, it may be difficult to discern a true minimum especially at the outlying areas where the concentrations are almost uniform.

k	x_k	y_k	q_k
1	0.721	0.637	0.176
2	0.812	0.243	0.412
3	0.175	0.320	0.412

Table 4.3: Locations and flux strengths of three capillaries reprised

Chapter 5

Discussion

The purpose of this dissertation is to provide a mathematical analysis of substrate diffusion for a multicapillary model which is different from the Krogh cylinder. The long and parallel multicapillaries lie inside a tissue region. Exchange of substrate between capillaries and tissue is fundamental in the function of most living creatures. Clustered multiple capillaries with arbitrary characteristics in a unit region i.e. rectangular, circular or with free boundary region were modeled in this paper. This is more natural than multicapillary arrays with homogeneous characteristics (e.g. location of single capillary, flux strength and unit region), due to the following reasons: 1. Heterogeneity is more common than homogeneity. For example, the Voronoi boundary usually does not form a repeated pattern. 2. The tissue region boundary is not an impermeable barrier and there are interactions among capillaries. Using uniform boundary conditions for each array cell may leave anoxic lethal corner. 3. Establishment of a perfused steady state for multicapillary supply region is naturally achieved from interaction between capillaries and readjustment of supply regions rather than substrate diffusion through single capillary-tissue unit boundaries.

The matching technique was first used in this paper to solve the governing equations for rectangular multicapillary regions. Neumann boundary was assumed and the a linear combination of eigenfunctions with unknown coefficients were used to express

the general solution. Then these coefficients were determined by using the matching conditions along the four boundary edges. Both of the steady state and transient state for such a region were solved. In the case of time-wise evolution of anoxia which occurs during the beginning state of diffusion, the capillary supply area forms hypoxic region which slowly vanishes at the tissue to regain its steady state. This process is much slower than the abolishment of such a state from sudden blockage or clamping one of the capillaries.

Except in special cases (e.g. Fig 1.3) the areas enclosed by each Voronoi polygon are of varied sizes. If Voronoi polygons also represent capillary supply areas, the capillary strengths, which are proportional to each area, would not be the same. Hoofd et al. [50] found the capillary supply areas are similar to Voronoi polygons. This is probably because in their simulation somewhat even strength and somewhat even distribution of capillaries are used, unlike the cases illustrated here. Clark et al. [55] used an image method to compute the concentration inside a circular region. Their results when computed are identical to Eq. (3.14). Hoofd [51] used a different boundary condition but his formulation is non-unique.

Since capillary length is about 10^2 times capillary diameter, in most cases the longitudinal diffusion of solute may be neglected in comparison to radial diffusion and therefore can be treated as a small perturbation to the solution. Eqs. (3.17) and (3.27) are solved implicitly for substrate solution inside the capillaries. The order of small perturbation is determined by the longitudinal location. At the both ends of the capillary cylinder, axial diffusion constant and radial diffusion constant are in the same order. Axial effect should to be treated differently and a full three dimensional analysis is required. Then the two set of solutions, describing oxygen diffusion in the cylinder and near the two ends of the cylinder, need to be matched completely to obtain the effect of axial diffusion.

Using insulated regions with regular boundaries such as rectangular and circular,

we found the general solutions for both steady and time-dependent unsteady states. The matching technique provides solutions in a fast convergent series form. Another research direction presented is the study of a diffusion-consumption model when the boundary is constantly moving(i.e. a Stefan problem). Using Fick's law of diffusion, the hexagonal compartmental model was used to describe two dimensional unsteady diffusion-consumption. The method models transport among cellular units and is much simpler than traditional finite differences.

Appendix A

Analytical Solution for Oxygen Distribution in Circular Domains

The solution to Eqs. (3.9) to (3.13) is in a general form

$$c_0(r,\theta,z) = r^2/4 + \sum_{j=1}^{N}\{C_{0,j} - \kappa/4 \cdot \ln \rho_j^2\} + \kappa \cdot \sum_{n=0}^{\infty} r^n (A_n \cos n\theta + B_n \sin n\theta) \qquad \text{(A.1)}$$

The first term is the particular solution due to uniform consumption. The second term is a combination of sources from each capillary. The last sum is the homogeneous solution which shall be treated using the matching technique similar to chapter 1.

The relation between ρ_j, φ_j and r θ is (Fig 3.2(b))

$$\rho^2 = r^2 + a_j^2 - 2ra_j \cos(\theta - \alpha_j) \qquad \text{(A.2)}$$

The coefficients A_n and B_n are determined by the boundary condition at $r = 1$.

The radial derivative of Eq.(A.1) is

$$\begin{aligned}\frac{\partial C}{\partial r} &= \frac{r}{2} - \kappa/4 \cdot \sum_{j=1}^{N} \frac{1}{\rho_j^2} \frac{\partial \rho_j^2}{\partial r} + \sum_{n=0}^{\infty} n r^{n-1}(A_n \cos n\theta + B_n \sin n\theta) \\ &= \frac{r}{2} - \kappa/4 \cdot \sum_{j=1}^{N} \frac{2r - 2a_j \cos(\theta - \alpha_j)}{r^2 + a_j^2 - 2ra_j \cos(\theta - \alpha_j)} \\ &\quad + \sum_{n=0}^{\infty} n r^{n-1}(A_n \cos n\theta + B_n \sin n\theta) \end{aligned} \tag{A.3}$$

At boundary there is no flux through

$$\sum_{n=0}^{\infty} n(A_n \cos n\theta + B_n \sin n\theta) = \frac{1}{2} - \kappa/2 \cdot \sum_{j=1}^{N} \frac{1 - a_j \cos(\theta - \alpha_j)}{1^2 + a_j^2 - 2a_j \cos(\theta - \alpha_j)} \tag{A.4}$$

Multiply Eq. (A.4) by $\cos(n\theta)$ and integrate from 0 to 2π gives

$$\kappa \cdot nA_n \pi = \kappa/2 \cdot \sum_{j=0}^{N} I_{j,n}, \qquad n \geq 1 \tag{A.5}$$

where

$$\begin{aligned} I_{j,n} &= \int_0^{2\pi} \frac{1 - a_j \cos(\theta - \alpha_j)}{1^2 + a_j^2 - 2a_j \cos(\theta - \alpha_j)} \cos(n\theta) d\theta \\ &= \int_0^{2\pi} \frac{1 - a_j \cos(\vartheta)}{1^2 + a_j^2 - 2a_j \cos(\vartheta)} \Big[\cos(n\vartheta)\cos(n\alpha_j) - \sin(n\vartheta)\sin(n\alpha_j) \Big] d\vartheta \\ &= 2\cos(n\alpha_j) \int_0^{\pi} \frac{1 - a_j \cos(\vartheta)}{1^2 + a_j^2 - 2a_j \cos(\vartheta)} \cos(n\vartheta) d\vartheta \\ &= \begin{cases} 2\pi, & n = 0 \\ \pi a_j^n \cos(n\alpha_j), & n \geq 1 \end{cases} \end{aligned} \tag{A.6}$$

Here $\theta = \theta - \alpha_j$ and we have used integration formulas from Gradshteyn and

Ryzhik[27]. Thus from Eq. (A.5)

$$A_n = \frac{1}{2n} \cdot \sum_{j=0}^{N} a_j^n \cos(n\alpha_j), \qquad n \geq 1 \tag{A.7}$$

Similarly multiply Eq. (A.4) by $\sin(n\theta)$ and integrate,

$$\kappa \cdot nB_n\pi = \kappa/2 \cdot \sum_{j=0}^{N} J_{j,n}, \qquad n \geq 1 \tag{A.8}$$

where

$$\begin{aligned} J_{j,n} &= \int_0^{2\pi} \frac{1 - a_j \cos(\theta - \alpha_j)}{1^2 + a_j^2 - 2a_j \cos(\theta - \alpha_j)} \sin(n\theta) d\theta \\ &= 2\sin(n\alpha_j) \int_0^{\pi} \frac{1 - a_j \cos(\vartheta)}{1^2 + a_j^2 - 2a_j \cos(\vartheta)} \cos(n\vartheta) d\vartheta \\ &= \begin{cases} 2\pi, & n = 0 \\ \pi a_j^n \sin(n\alpha_j), & n \geq 1 \end{cases} \end{aligned} \tag{A.9}$$

Thus

$$B_n = \frac{1}{2n} \cdot \sum_{j=0}^{N} a_j^n \sin(n\alpha_j), \qquad n \geq 1 \tag{A.10}$$

Details and examples can also be found in [12].

Appendix B

Substrate Distribution within Capillaries

To find the solution of $C_0(z)$ to Eq. (3.12), substitute $c_0(r,\theta,z)$ (3.14) into (3.12).

$$\frac{d}{dz}[C_0 + VS(C_0)] = \gamma \int_0^{2\pi} \frac{\partial}{\partial \rho}(c_{0,p} + c_{0,s} + c_{0,h})\Big|_{\rho=R} d\phi \tag{B.1}$$

where $c_{0,p}$ is the particular solution, $c_{0,s}$ is the combination of capillary source solutions and $c_{0,h}$ is the homogeneous solution.

$$c_{0,p} = (\rho_j^2 + a_j^2 - 2a_j\rho_j\cos(\phi))/4 \tag{B.2}$$

$$c_{0,s} = \sum_{j=1}^{N}[C_{0,j}(z) - \kappa/2 \cdot \ln(\rho_j)] \tag{B.3}$$

$$c_{0,h} = \sum_{n=0}^{\infty} r^n(A_n\cos n\theta + B_n \sin n\theta) \tag{B.4}$$

where A_n and B_n are constant coefficients

$$A_n = \frac{\kappa}{2n}\sum_{j=1}^{N} a_j^n \cos(n\alpha_j), \quad B_n = \frac{\kappa}{2n}\sum_{j=1}^{N} a_j^n \sin(n\alpha_j), \quad for\ \ n \geq 1 \tag{B.5}$$

In order to find the right hand side of Eq. (B.1), we proceed

$$\begin{aligned}\int_0^{2\pi} \frac{\partial c_{0,p}}{\partial \rho_j}\Big|_{\rho_j=R} d\phi &= 1/4 \int_0^{2\pi} \frac{\partial}{\partial \rho_j}\Big(\rho_j^2 + a_j^2 - 2a_j\rho_j\cos(\phi)\Big)\Big|_{\rho_j=R} d\phi \\ &= 1/2 \int_0^{2\pi} \Big(R - a_j\cos(\phi)\Big)\, d\phi \\ &= R\cdot\pi \end{aligned} \tag{B.6}$$

$$\begin{aligned}\int_0^{2\pi} \frac{\partial c_{0,s}}{\partial \rho_j}\Big|_{\rho_j=R} d\phi &= \sum_{j=1}^{N} \int_0^{2\pi} \frac{\partial}{\partial \rho_j}\Big(C_{0,j}(z) - \kappa/2\cdot\ln(\rho_j)\Big)\Big|_{\rho_j=R} d\phi \\ &= -\kappa/R\cdot\pi - \kappa/4 \sum_{i\neq j} \int_0^{2\pi} \frac{\partial}{\partial \rho_j}\ln(\rho_i^2)\Big|_{\rho_j=R} d\phi \\ &= -\kappa/R\cdot\pi - \kappa/4 \sum_{i\neq j} \int_0^{2\pi} \frac{1}{\rho_i^2}\frac{\partial \rho_i^2}{\partial \rho_j}\Big|_{\rho_j=R} d\phi \\ &= -\kappa/R\cdot\pi - \kappa/2 \sum_{i\neq j} \int_0^{2\pi} \frac{R - \widehat{a}_j\cos\widehat{\phi}}{R^2 + \widehat{a}_j^2 - 2R\widehat{a}_j\cos\widehat{\phi}}\, d\widehat{\phi} \\ &= -\kappa/R\cdot\pi - \kappa/2 \sum_{i\neq j} 2\pi \end{aligned} \tag{B.7}$$

Here we have used integration formula from Gradshteyn and Ryzhik [27]. Thus

$$\int_0^{2\pi} \frac{\partial c_{0,s}}{\partial \rho_j}\Big|_{\rho_j=R} d\phi = -\kappa/R\cdot\pi - N\pi = -\pi\cdot\left(\frac{\kappa}{R} + N\right) \tag{B.8}$$

For the last term on the right hand side of Eq. (B.1)

$$\begin{aligned}\int_0^{2\pi} \frac{\partial c_{0,h}}{\partial \rho_j}\Big|_{\rho_j=R} d\phi &= \sum_{j=1}^{N}\sum_{n=1}^{\infty} \int_0^{2\pi} \frac{\partial}{\partial \rho_j} r^n (A_n\cos n\theta + B_n\sin n\theta)\Big|_{\rho_j=R} d\phi \\ &= \sum_{j=1}^{N}\sum_{n=1}^{\infty} \frac{\kappa}{2n} \int_0^{2\pi} \frac{\partial}{\partial \rho_j} r^n\, a_j^n\, \cos n(\theta - \alpha_j)\Big|_{\rho_j=R} d\phi \end{aligned} \tag{B.9}$$

For $n = 1$

$$\begin{aligned}\frac{\kappa}{2}\int_0^{2\pi}\frac{\partial}{\partial\rho_j} r\,a_j\,\cos(\theta-\alpha_j)\Big|_{\rho_j=R} d\phi &= \frac{\kappa}{4}\int_0^{2\pi}\frac{\partial}{\partial\rho_j}(r^2+a_j^2-2\rho_j^2)\Big|_{\rho_j=R} d\phi \\ &= \frac{\kappa}{2}\int_0^{2\pi}\frac{\partial}{\partial\rho_j}(a_j^2-\rho_j a_j\cos\phi)\Big|_{\rho_j=R} d\phi \\ &= -\frac{\kappa}{2}\int_0^{2\pi} a_j\cos\phi\,d\phi \\ &= 0 \end{aligned} \tag{B.10}$$

For $n = 2$

$$\begin{aligned}&\frac{\kappa}{4}\int_0^{2\pi}\frac{\partial}{\partial\rho_j} r^2\,a_j^2\,\cos 2(\theta-\alpha_j)\Big|_{\rho_j=R} d\phi \\ &= \frac{\kappa}{4}\int_0^{2\pi}\frac{\partial}{\partial\rho_j}\left(2r^2\,a_j^2\cos^2(\theta-\alpha_j)-r^2\,a_j^2\right)\Big|_{\rho_j=R} d\phi \\ &= \frac{\kappa}{4}\int_0^{2\pi}\frac{\partial}{\partial\rho_j}\left(2(a_j^2-\rho_j a_j\cos\phi)^2-(\rho_j^2+a_j^2-2\rho_j a_j\cos\phi)\,a_j^2\right)\Big|_{\rho_j=R} d\phi \\ &= \frac{\kappa}{2}\int_0^{2\pi}\left(2(a_j^2-Ra_j\cos\phi)(-a_j cos\phi)-(R-a_j\cos\phi)\,a_j^2\right) d\phi \\ &= \frac{\kappa}{2}\,R\,a_j^2\left(\int_0^{2\pi}(\cos 2\phi+1)\,d\phi\right) \\ &= \kappa\pi a_j^2 \end{aligned} \tag{B.11}$$

for $n \geq 3$, the nth order in the $c_{0,h}$ series representation has partial derivative of order $o(R)$. Therefore combine the results all above

$$\frac{d}{dz}[C_0 + VS(C_0)] = \pi\gamma\,(R - \frac{\kappa}{R} - N) + \widehat{\varphi_0}(R) \tag{B.12}$$

where

$$\widehat{\varphi_0}(r) = \sum_{j=1}^{N} a_j^2\kappa\cdot\pi r + O(r^2) \quad for \quad r \ll 1 \tag{B.13}$$

Bibliography

[1] A.Krogh, The number and distribution of capillaries in muscles with calculations of the oxygen pressure head necessary for supplying the tissue, *J.Physiol.*, 52 1919.

[2] A. Apelblat, A. Katzir-Katchalsky, and A. Silberberg, A mathematical analysis of capillary-tissue fluid exchange, *Biorheology*, 11:1-49 1974.

[3] A.E. Berga, M. Ciment, and J.C.W. Rogers, Numerical solution of a diffusion consumption problem with a free boundary,*SIAM J. Num. Anal.*, 12:646-672 , 1975.

[4] A. Heimdal and H. Torp. Ultrasound doppler measurements of low velocity blood flow: Limitations due to clutter signals from vibrating muscles. *IEE Trans. Ultrason. Ferroelect. Freq. Contr.*, 44:873-880 , 1997.

[5] A.S. Popel, Theory of oxygen transport to tissue, *Crit. Rev. Biomed. Eng.*, 17, 257, 1989.

[6] A.S. Popel, C.K. Charny and A.S. Dvinsky, Effect of heterogeneous oxygen delivery on the oxygen distribution in skeletal muscle, *Math. Biosci.* , 81:91-113, 1986.

[7] A.S. Popel, Oxygen diffusive shunts under conditions of heterogeneous oxygen delivery, *J. Theor. Biol.*, 96 533, 1982.

[8] A.S. Popel, Analysis of capillary-tissue diffusion in multicapillary systems. *Math. Biosci.*, 39:187-211, 1978.

[9] B. Klitzman, A.S. Popel, and B.R. Duling, Oxygen transport in resting and contracting cremaster muscles: experimental and theoretical microvascular studies, *Microvasc. Res.*, 25: 108-131 1983.

[10] B. Chance, B. Schoener, and F. Schlindler, In Oxygen in the animal organism, F. Dickens and E. Neil, eds., 367-388. Pergamon, Oxford, 1964.

[11] B.A. Taylor and J.D. Murray, Effects of the rate of oxygen consumption on muscle respiration.*J. Math. Biology.*, 4:1-20, 1976.

[12] C.Y. Wang, J.B. Bassingthwaighte, Capillary supply regions, *Math. Biosci.*, 173 103, 2001.

[13] D.F. Bruley and H.I. Bicher, Oxygen transport to tissue, *Advances in Experimental Medicine and Biology*, Vol. 37B, Plenum, New York, 1973.

[14] D.D. Reneau, E.J. Guilbeau, R.E. Null, Oxygen dynamics in the brain. *Microvasc. Res.*, 13: 357, 1977.

[15] D.D. Reneau, E.J. Guilbeau, J.M. Cameron, A theoretical analysis of the dynamics of oxygen transport and exchange in the placental-fetal system *Microvasc. Res.*, 8: 346, 1974.

[16] D.D. Reneau, D.F. Bruley, and M.H.Knisely, A mathematical simulation of oxygen release, diffusion and consumption in the capillaries and tissue of the human brain. *Chemical Engineering in Medicine and Biology*, New York, 1967.

[17] D. Goldman and A.S. Popel, A computational study of the effect of capillary network anastomoses an tortuosity on oxygen transport, *J. Theor. biol.*, 206:181-194 , 1980.

[18] E. Opitz and M. Schneider, The oxygen supply of the brain and the mechanism of deficiency effects,*Ergeb. Physiol. Biol. Chem. Exptl. Pharmakol.*, 46: 126-260,1950

[19] E.P. Salathe, Mathematical analysis of oxygen concentration in a two dimensional array of capillaries, *J. Math. biol.*, 2002.

[20] E.P. Salathe, and C.Chen. The role of myoglobin in retarding oxygen depletion in skeletal muscle, *Math. Biosci.*, 116: 1-20, 1993.

[21] E.P. Salathe, and Y.H. Xu, Mathematical analysis of transport and exchange in skeletal muscle, *Proc. R. Soc. Lond.*, B324: 303-318 1988.

[22] E.P. Salathe, and R.W. Kolkka, Reduction of anoxia through myoglobin facilitated diffusion of oxygen, *biophys. J.*, 50: 885-894 1986.

[23] E.P. Salathe, T-C. Wang, The development of anoxia following occlusion, Bull. *Math. Biol.*,44 851 , 1982.

[24] E.P. Salathe and T-C. Wang, J.F. Gross, Mathematical analysis of oxygen transport to tissue. *Math biosci.*, 49: 235-247, 1980.

[25] G.J. Fleishman. T.W.Secomb, J.F. Gross, Effect of extravascular pressure gradients on capillary fluid exchange. *Math. Biosci*, 81:145-164, 1986.

[26] G.N. Watson, A treatise on the theory of Bessel Functions, 2nd ed. Cambridge University Press, Cambridge, 1952.

[27] I.S. Gradshteyn, I.M. Ryzhik, Tables of Integrals Series and Products, 5th ed., Academic Press, San Diego, CA, 1994.

[28] J. Crank, The mathematics of diffusion, 2nd Ed. Clarendon, Oxford, 1975

[29] J. Go, Oxygen Delivery through Capillaries,*Math. Bio.*, 208:166-176, 2007

[30] J.B. Wittenberg, Myoglobin facilitated oxygen diffusion: Role of myoglobin in oxygen entry into the muscle,*Physiol. Rev.*, 50(4):559-635, 1970.

[31] J.E. Fletcher. On facilitated oxygen diffusion in muscle tissues, *Biophys. J.*, 29:437-458, 1980.

[32] J.E. Fletcher, Mathematical modeling of the microcirculation, *Math. Biosci*, 38,159, 1978.

[33] J.E. Fletcher. Some model results on hemoglobin kinetics and its relationship to oxygen transport in blood. In Advances in Experimental Medicine and Biology, 75. Grote. Reneau and Thews. Eds. Plenum Press, New York and London , 1976.

[34] J.E. Fletcher. A model describing the unsteady transport of substrate to tissue from the microcirculation. *SIAM J. Appl. Math*, 29(3):449 , 1975.

[35] J.E. Fletcher, A mathematical model of the unsteady transport of oxygen to tissue in the microcirculation. In Advances in Experimental Medicine and Biology, 37B. Bruley, Bicher, eds. Plenum Press, New York and London, 1973.

[36] J.D. Murray, Mathematical Biology. Biomathematics Texts 19. Berlin: Heidelberg, springer-Verlag, 1989.

[37] J.D. Murray, Lectures on nonlinear Differential Equation Models in Biology. Oxford University Press, , 1978.

[38] J.D. Murray, On the role of myoglobin in muscle respiration.*J. Theor. Biol*, 47:115-126, 1974.

[39] J.D. Murray, On the molecular mechanism of facilitated oxygen diffusion of hemoglobin and myoglobin. *Proc. R. Soc. Lond. B Biol*,178:95-110 , 1971.

[40] J.J. Blum. Concentration profiles in and around capillaries. *Amer. J. Physiol.*, 198:991-998 , 1960.

[41] J.F. Gross and J. Aroesty, The mathematics of capillary flow: A critical review *Biorheology*, 9:225-264 1972.

[42] J.M. Gonzalez-Fernandez, S.E. Atta, Concentration of oxygen around capillaries in polygonal region of supply, *Math. Biosci.*, 13 55 1972.

[43] J. Prothero and A.C. Burton, The physics of blood flow in capillaries, I,*biophys. J.*, 1:565-578 , 1961.

[44] J.P. Whiteley and D.J. Gavaghan, C.E.W. Hahn, Mathematical modeling of oxygen transport to tissue. *J. Math. Biol.*, , 2002.

[45] J.W. Brown, R.V.Churchill, Frourier series and boundary value problems, 5^{th} ed , Megraw-Hill, Inc. 1993.

[46] K. Schmidt-Nielsen, P. Pennycuik, Capillary density in mammals in relation to body size and oxygen consumption *Amer. J. Physiol.*, 200:746-760, 1961.

[47] L. Hoofd. Calculation of oxygen pressures in tissue with anisotropic capillary orientation. I. Two-dimensional analytical solution for arbitrary capillary characteristics. *Math Biosci.* 129:1-23 , 1995.

[48] L. Hoofd. Calculation of oxygen pressures in tissue with anisotropic capillary orientation. II. Coupling of two-dimensional planes.*Math Biosci*, 129:25-39, 1995.

[49] L. Hoofd, Z.Turek, The influence of flow redistribution on the calculated PO_2 in rat heart tissue, in oxygen transport to tissue XV, Advances in Experimental Medicine and Biology, 345. P.Vaupel, R.Zander and D.F.Bruley. eds. Plenum Press, New York and London pp 275-282 , 1990.

[50] L. Hoofd, Z. Turek, J. Olders, Calculation of oxygen pressures and fluxes in a flat plane perpendicular to any capillary distribution, In Oxygen Transport to Tissue XIAdv. Exp. Med. Biol., 248 187, 1989.

[51] L. Hoodfd, Z. Turek, K.Kubat, B.E.M. Ringnalda, S.Kazda, Variability of intercapillary distance estimated on histological sections of rat heart, In F. Kreuzer et al. eds, Oxygen Transport to Tissue VII, Adv. Exp. Med. Biol. 191-239, 1985.

[52] M.M. Lih, Transport Phenomena in Medicine and Biology. John Wiley Sons, New York, London, Sydney and Toronto, , 1975.

[53] M. Sharan, B. Singh, M.P. Singh and P.Kumar, Finite-element analysis of oxygen transport in the systemic capillaries. *IMAJ. Math. Appl. Biol. and Med.*, 8:107-123, 1991.

[54] N.T.S. Evans, and A.A. Gourlay, The solution of a two-dimensional time-dependent diffusion problem concerned with oxygen metabolism in tissues, *J. Inst. Math Appl.*, 19:239-251, 1977.

[55] P.A. Clark, S.P. Kennedy, A. Clark Jr., Buffering of muscle tissue in PO_2 levels by the oxygen field from many capillaries, IN Oxygen Transport to Tissue XI, Adv. Exp. Med. Biol., K. Rakusan et al. eds, 248, 165, 1989.

[56] P.F. Scholander, Oxygen transport through hemoglobin solutions,*Science*, 131:585-590 , 1980.

[57] R.Hsu, T.W. Secomb, A green's function method for analysis of oxygen delivery to tissue by microvascular networks. *Math Biosci.*, 96:61-78 , 1989.

[58] R. W. Kolkka and E. P. Salathe. A mathematical analysis of carrier-facilitated diffusion, *Math Biosci.*, 71:147-179 , 1984.

[59] R.W. Schubert and Z. Zhang, The equivalent Krogh cylinder and axial oxygen transport. Oxygen Transport to Tissue XVIII, 191-202 , 1997.

[60] S. Egginton, Morphometric analysis of tissue capillary supply, In R.G. Boulilier eds, Adv. Comp. Environ. Physiol., Vol 6, Springer, Berlin, 1990.

[61] S.S. Kety, Determinants of tissue oxygen tension,*Federation Proc.*, 16:666-670, 1957.

[62] S. Middleman, Transport phenomena in the cardiovascular system, Wiley-Interscience, New York, 1972.

[63] V. Riveros-Moreno, J.B. Wittenberg, The self-diffusion coefficients of myoglobin and haemoglobin in concentrated solution. *J.Biol. Chem.* 247:895-901 , 1972.

[64] W. A. Hyman, Asimplified model of the oxygen supply function of capillary blood flow. In Advances in Experimental Medicine and Biology, 37B. Bruley and Bicher, eds, Plenum Press, New York and London, 1973.